

# Opportunistic Routing Aided Cooperative Communication MRC Network With Energy-Harvesting Nodes

LEI TENG<sup>1</sup>, WANNIAN AN<sup>1</sup>, CHEN DONG<sup>1</sup>, XIAODONG XU<sup>1</sup> (Senior Member, IEEE),  
AND BOXIAO HAN<sup>2</sup>

<sup>1</sup>School of Information and Communication Engineering, Beijing University of Posts and Telecommunications, Beijing 100088, China

<sup>2</sup>Future Mobile Technology Lab China Mobile Research Institute, Beijing, China

CORRESPONDING AUTHOR: C. DONG (e-mail: dongchen@bupt.edu.cn)

This work was supported in part by the State Key Laboratory of Networking and Switching Technology, Beijing University of Posts and Telecommunications and in part by the Beijing University of Posts and Telecommunications-China Mobile Research Institute Joint Innovation Center under Project R207010101125D9.

**ABSTRACT** In this research, we present a cooperative communication network based on two energy-harvesting (EH) decode-and-forward (DF) relays that contain the harvest-store-use (HSU) architecture and may harvest energy from the surrounding environment by utilizing energy buffers. To improve the performance of this network, an opportunistic routing (OR) algorithm is presented that takes into account channel status information, relay position, and energy buffer status, as well as using the maximal ratio combining (MRC) at the destination to combine the signals received from the source and relays. The theoretical expressions for limiting distribution of energy stored in infinite-size buffers are derived from the discrete-time continuous-state space Markov chain model (DCSMC). In addition, the theoretical expressions for outage probability, throughput, and per-packet time slot cost in the network are obtained utilizing both the limiting distributions of energy buffers and the probabilities of transmitter candidates set. Through numerous simulation results, it is demonstrated that simulation results match with corresponding theoretical results.

**INDEX TERMS** Energy-harvesting, opportunistic routing, maximal ratio combining, state transition matrix.

## I. INTRODUCTION

IN RECENT years, due to the emphasis on green communications, there has been a great deal of interest in EH technique, which can harvest energy from the surrounding ambient sources such as radio frequency energy, light energy, thermal energy [1]. In addition to the advantages of energy saving, EH can also extend battery lifetime compared to the source charging the battery, which is helpful in the complicated case of replacing the battery [2]. For these reasons, numerous articles emphasize the combination of EH and communication.

In [3], a relay selection approach for the EH wireless body area network that takes into account both channel state information (CSI) and the energy condition of the relay buffer is proposed. For the sake of obtaining a tradeoff between the transmission energy and decoding

energy, the power splitting protocol is employed at the EH relay of the EH-based cooperative communication network in [4] and [5]. In these papers, the harvest-use (HU) architecture is employed to manage energy, meaning that the node will instantly use the gathered energy.

On the other hand, the harvest-store-use (HSU) architecture, which is widely explored as an efficient technique of energy harvesting from the environment, is comprised of three energy management steps: energy harvesting, energy storage, and energy use. In [6], a simple communication system with EH using HSU architecture is proposed, assuming that the EH node harvests energy from a radio frequency signal broadcast by an access point in the downlink and uses the stored energy to transmit data in the uplink. Unlike [6], which only investigated the on-off policy, both the best-effort policy and the on-off policy are analyzed in [7]. Both [6]

and [7] derived the limiting distribution of stored energy in the energy buffer at the EH node by using the theory of discrete-time continuous-state Markov chains. The difference between the on-off policy and the best-effort policy is whether set target energy to transmit information or not. In the on-off policy, only when target  $M$  units of energy are available in the energy buffer, the EH node can transmit information to the destination at the cost of  $M$  units of energy. In the best-effort policy, no matter how much energy is in the energy buffer, the EH node uses all the energy to transmit information to the destination. To maximize the end-to-end system throughput under data and energy storage constraints, the online and offline optimization algorithms for joint relay selection and power control have been discussed in [8]. A buffer-aided adaptive wireless powered communication network with finite energy storage and data buffer is proposed in [9], which can fully exploit the temporal diversity gains, while the weighted max-min fair access design can effectively ensure the fair access requirements by different users with some loss in the achieved sum-rate.

In the aforementioned papers, all EH nodes harvest energy from RF signals received from the downlink, which is not efficient when the path loss in practical communication links is high. And they only consider the relay link without a direct link. The self-sustaining node (SSN), which harvests energy from the ambiance, is regarded as a solution to the high path loss link in the EH network. Self-sustaining node and direct link are covered in [10], where the limiting distributions of energy for both the incremental on-off policy and the incremental best-effort policy are derived by using a discrete-time continuous-state space Markov chain. In addition, the expressions for outage probability and throughput are obtained. In this process, the maximal ratio combining technique is used to improve the performance of the network. In all of the papers mentioned above, each source node in the cooperative relay network is powered by a power source. For the sake of further energy saving, the source node is equipped with the EH technique in [11]. A networks with an energy buffer-aided source and a data buffer-Aided relay is proposed in [12], which uses discrete-time continuous-state Markov chain model to model the energy buffer. A decoded-and-forward energy-harvesting system with multiple relays in the presence of transmitting hardware impairments is proposed in [13]. The system has two transmitting policies. For policy-1, the selection of the best relay that assists the source-to-destination communication is based on the first-hop channel-state-information. For policy-2, the selection of the best relay is based on the second-hop CSI.

All relay networks mentioned above are primarily founded on wireless two-hop relay networks with a single relay or multiple relays with the same priority. However, in reality, a practical wireless cooperative network, such as a wireless sensor network [14] or an Internet of Things (IoT) network [15], is a wireless multi-hop network. Opportunistic routing as a solution to improve the performance of the wireless multi-top network has been widely studied [16]. An

TABLE 1. Comparison of references.

Reference	EH buffer architecture	SSN	OR	MRC
[3],[4],[5]	HU	N	N	N
[6],[7],[8],[9]	HSU	N	N	N
[10],[11]	HSU	Y	N	Y
[12],[13]	HSU	Y	N	N
[16],[17],[18]	No EH	N	Y	N
[19]	HSU	Y	Y	N
[20]	No EH	N	N	Y
Our work	HSU	Y	Y	Y

energy-efficient OR, which exploits cross-layer information exchange and energy-consumption-based objective functions, is proposed in [17] and [18] where it has been clarified that OR outperforms traditional routing with the specific pre-selected route in terms of system performance. And in [19], with using OR algorithm, a cooperative communication network based on two energy-harvesting decode-and-forward relays is proposed.

According to the above researches, maximal-ratio combining as a well-studied technique [20], which is helpful to improve performance in communication networks, is worth being combined with EH. This article is targeted at proposing and designing an analytical framework for the study of OR-aided cooperative communication networks with EH nodes and using MRC in our system. Table 1 shows the comparison between our work and the above references, where N indicates that the technology is not employed in the studied system, and Y indicates that the technology is employed in the studied system. In addition, we model energy buffers using discrete-time continuous-state space Markov chains. The contributions of this work are as follows:

- 1) A cooperative network consisting of two EH DF relay nodes and employing the MRC and OR algorithms is proposed.
- 2) The expressions for the limiting distributions of energy stored in buffers are obtained with the help of the DCSMC model and the state-transition-matrix-based (STM) theoretical solutions of the probability of transmitter candidates set. The limiting distributions of energy are the base of further analysis.
- 3) A algorithm is given to calculate the probability density function of the received SNR of the destination node under the condition of each transmitter candidates set by using the Markov state transition matrix.
- 4) The closed-form expressions of outage probability and throughput are derived.
- 5) Through numerous simulation results, it is demonstrated that simulation results match with corresponding theoretical results.

The remaining paper is developed as follows: Section II interprets the system model and OR protocol. In section III, the limiting PDFs of the energy stored in the buffers R1 and R2 are presented. In Section IV, the expressions for outage

TABLE 2. Notations table.

Notation	Meaning
$A \sim \mathcal{CN}(0, \theta)$	the random variable $A$ follows the complex Gaussian distribution with mean 0 and variance $\theta$
$ B $	the absolute value of $B$
$\mathbb{E}[\cdot]$	the expectation operator
$C_1 \cup C_2$	the union of the condition $C_1$ and the condition $C_2$
$C_1 \cap C_2$	the intersection of the condition $C_1$ and the condition $C_2$
$W(\cdot)$	the Lambert W function
<b>Boldface capital T</b>	matrices or vectors
$\overline{\mathbb{C}}$	the complementary event of $\mathbb{C}$
*	multiplication
	conditional probability. For example, case A,B—C means event A and B occur under the condition of C.
$\text{conv}(A, B)$	discrete convolution $y(j) = \text{conv}(A, B) = \sum_{i=-\infty}^{+\infty} A(i)B(j-i)$

TABLE 3. Abbreviations table.

Abbreviation	Meaning
EH	energy harvesting
DF	decode and forward
HSU	harvest-store-use
OR	opportunistic routing
MRC	maximal ratio combing
DCSMC	discrete-time continuous-state space Markov chain
CSI	channel state information
HU	harvest-use
SSN	self-sustaining node
PEB	primary energy buffer
SEB	secondary energy buffer
ACK	positive acknowledgement
NACK	negative acknowledgement
TC	transmitter candidate

probability and throughput are determined. In Section V, simulation performance results are displayed. Section VI is where the conclusion is provided.

*Notations:* In Table 2, all notations are showed.

*Abbreviation:* In Table 3, all abbreviations are showed.

## II. SYSTEM MODEL AND OR PROTOCOL

### A. SYSTEM MODEL

As shown in Fig. 1, the network proposed in this paper is composed of a source node S, two DF relay nodes R1 and R2, and a destination node D. All nodes are assumed as half-duplex nodes. Only the source and destination nodes are powered by the power supply, while relay nodes are equipped with energy buffers using HSU architectures to harvest ambient energy. In each time slot, only one node is activated and can transmit signals by broadcast way, while others are silent or receive the signals. Quasi-static Rayleigh fading is assumed between all nodes. Let  $d_{ab}$

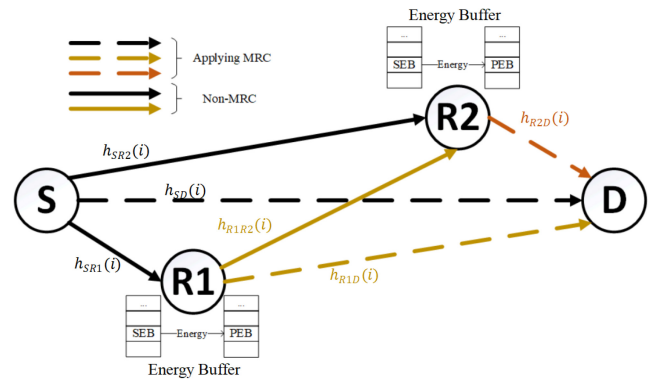


FIGURE 1. System model.

denote the distance between nodes with a and b. Hence, denoted by  $h_{SD}(i) \sim \mathcal{CN}(0, d_{SD}^\alpha)$ ,  $h_{SR1}(i) \sim \mathcal{CN}(0, d_{SR1}^\alpha)$ ,  $h_{SR2}(i) \sim \mathcal{CN}(0, d_{SR2}^\alpha)$ ,  $h_{R1R2}(i) \sim \mathcal{CN}(0, d_{R1R2}^\alpha)$ ,  $h_{R1D}(i) \sim \mathcal{CN}(0, d_{R1D}^\alpha)$  and  $h_{R2D}(i) \sim \mathcal{CN}(0, d_{R2D}^\alpha)$  the channel coefficients within the  $i$ -th time slot between S and D, S and R1, S and R2, R1 and R2, R1 and D, and R2 and D respectively, where the term  $\alpha$  represents the path-loss exponent.

The HSU architectures equipped by the relay nodes mainly have two energy buffers respectively, which are an infinite-size primary energy buffer (PEB) and an infinite-size secondary energy buffer (SEB), for the reason that storage devices are disabled to charge and discharge at the same time [21], [22]. The energy harvested from ambiance is stored in SEB first. Then, in order to make the energy buffer equipped by relay nodes R1 and R2 charge and discharge simultaneously, SEB transfers the energy to the PEB at the end of each time slot. Finally, the energy in PEB is used to power the node to transmit signals. Due to the fact that the energy harvesting power is far smaller than the actual energy buffer capacity, the capacity of the energy buffer is considered to be infinite size in the theoretical analysis. In [22], it is indicated that there is no energy loss during charging between SEB and PEB or discharging between PEB and the node transmitter. The signals received from S, R1, and R2 are combined using MRC at D.

The source S broadcasts unit-energy symbols  $x_S(i)$  to relay R1, relay R2, and destination D at rate  $R_0$  with the constant power  $P_S$ . The received signals  $y_{SR1}(i)$ ,  $y_{SR2}(i)$  and  $y_{SD}(i)$  at relay R1, relay R2 and destination D in the  $i$ -th time slot are given by

$$y_{SR1}(i) = \sqrt{P_S}h_{SR1}(i)x_S(i) + n_{SR1}(i), \quad (1)$$

$$y_{SR2}(i) = \sqrt{P_S}h_{SR2}(i)x_S(i) + n_{SR2}(i), \quad (2)$$

$$y_{SD}(i) = \sqrt{P_S}h_{SD}(i)x_S(i) + n_{SD}(i), \quad (3)$$

where,  $n_{SR1}(i)$ ,  $n_{SR2}(i)$  and  $n_{SD}(i) \sim \mathcal{CN}(0, N_0)$  represent the received additive white Gaussian noise (AWGN) at R1, R2 and D, respectively. Thus, the received signal-to-noise ratios (SNRs)  $\gamma_{SR1}(i)$ ,  $\gamma_{SR2}(i)$  and  $\gamma_{SD}(i)$  at R1, R2 and D

in the  $i$ -th time slot would be given as follows

$$\gamma_{SR1}(i) = \frac{P_S |h_{SR1}(i)|^2}{N_0}, \quad \gamma_{SR2}(i) = \frac{P_S |h_{SR2}(i)|^2}{N_0}$$

and  $\gamma_{SD}(i) = \frac{P_S |h_{SD}(i)|^2}{N_0}$ . (4)

As a DF relay, the relay R1 decodes the received signals, re-encodes them into unit-energy symbols  $x_{R1}(i)$ , and then broadcasts  $x_{R1}(i)$  to relay R2 and destination D with the constant power  $M_{R1}$ . Similarly, the relay R2 obtains the unit-energy symbols  $x_{R2}(i)$  in the same way as relay R1, and then transmits  $x_{R2}(i)$  to the destination D with the constant power  $M_{R2}$ . Next, the received signals  $y_{R1R2}(i)$ ,  $y_{R1D}(i)$  and  $y_{R2D}(i)$  at relay R2 and destination D in the  $i$ -th time slot can be represented by

$$y_{R1R2}(i) = \sqrt{M_{R1}} h_{R1R2}(i) x_{R1}(i) + n_{R1R2}(i), \quad (5)$$

$$y_{R1D}(i) = \sqrt{M_{R1}} h_{R1D}(i) x_{R1}(i) + n_{R1D}(i), \quad (6)$$

$$y_{R2D}(i) = \sqrt{M_{R2}} h_{R2D}(i) x_{R2}(i) + n_{R2D}(i), \quad (7)$$

where,  $n_{R1R2}(i)$ ,  $n_{R1D}(i)$  and  $n_{R2D}(i) \sim \mathcal{CN}(0, N_0)$  denote the received AWGN at R2 and D, respectively. Similarly, the received SNRs  $\gamma_{R1R2}(i)$ ,  $\gamma_{R1D}(i)$  and  $\gamma_{R2D}(i)$  at R2 and D can be expressed as follows

$$\gamma_{R1R2}(i) = \frac{M_{R1} |h_{R1R2}(i)|^2}{N_0}, \quad \gamma_{R1D}(i) = \frac{M_{R1} |h_{R1D}(i)|^2}{N_0}$$

and  $\gamma_{R2D}(i) = \frac{M_{R2} |h_{R2D}(i)|^2}{N_0}$ . (8)

According to channel assumption, the PDF of SNR of channel SR1, SR2, SD, R1D, R1R2 and R2D can be expressed as  $f_{Node1Node2}(x) = W_{Node1Node2} e^{-W_{Node1Node2} x}$ .

For example, the PDF of SNR of channel SR1 can be expressed as  $f_{SR1}(x) = W_{SR1} e^{-W_{SR1} x}$ , where,  $W_{SD} = \frac{d_{SD}^\alpha N_0}{P_S}$ . Similarly,  $W_{SR2} = \frac{d_{SR2}^\alpha N_0}{P_S}$ ,  $W_{SR1} = \frac{d_{SR1}^\alpha N_0}{P_S}$ ,  $W_{R1D} = \frac{d_{R1D}^\alpha N_0}{M_{R1}}$ ,  $W_{R1R2} = \frac{d_{R1R2}^\alpha N_0}{M_{R1}}$ ,  $W_{R2D} = \frac{d_{R2D}^\alpha N_0}{M_{R2}}$ .

Let

$$\Gamma_{th} = 2^{R_0} - 1 \quad (9)$$

be the network SNR threshold, where  $R_0$  represents the target data transmitting rate.

In our system, a whole time slot is divided into four sub slots as shown in Fig. 2, where a whole time slot consists of pilot broadcasting sub-slot  $t_1$ , signalling broadcasting sub-slot  $t_2$ , packet broadcasting sub-slot  $t_3$  and positive acknowledgement (ACK) or negative acknowledgement (NACK) broadcasting sub-slot  $t_4$ . In sub-slot  $t_1$ , node D and relay nodes R1 and R2 need to broadcast the pilot signals sequentially, allowing each node to determine the CSI between itself and other nodes. Moreover, the pilot signal of D carries the overall SNR  $\gamma_{overall}$  of the current received packet combined by the MRC technique so that S, R1, and R2 nodes can know the current SNR threshold  $\Gamma_{th} - \gamma_{overall}$ . About  $\gamma_{overall}$  is described in OR protocol. In sub-slot  $t_2$ , each node determines whether it is able to transmit the

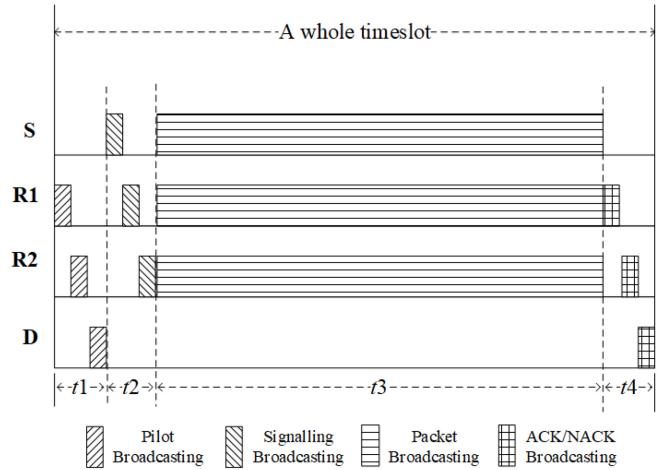


FIGURE 2. Time slot model.

packet depending on its energy state, CSI and ownership of the packet. If the node can transmit the packet, then it broadcasts high-level signalling; otherwise, it broadcasts low-level signalling. And the order of S, R1, and R2 signalling broadcasting is shown in Fig. 2. In this way, each node can obtain the transmission state of the cooperative network. In sub-slot  $t_3$ , with the transmission state, nodes determine whether transmit the packet or not based on the OR protocol described below. Then only one node can broadcast the packet in sub-slot  $t_3$ . The blocks of sub-slot  $t_3$  shown in Fig. 2 just means that S, R1, and R2 are all able to broadcast packet in sub-slot  $t_3$ , but do not mean that they can broadcast packet at the same time slot. In sub-slot  $t_4$ , D, R1, and R2 send a positive acknowledgment or a negative acknowledgment to indicate their reception statuses. Only when the instantaneous link SNR at the receiving node is not less than the threshold  $\Gamma_{th}$ , ACK signals would be broadcasted by the receiving node as the sign of successful packet reception.

## B. OR PROTOCOL

In this part, the main steps implemented by the OR protocol are described. S, R1, and R2 are broadcast nodes. There can be more than one broadcast node as transmitter candidates (TC) at the same time which have the packet. TC set at the  $i$ -th time slot is denoted by  $TCs(i)$ . The node which can receive the signals transmitted by the broadcast node is named the neighboring node of the broadcast node. Thus, in this system, neighboring nodes of S are R1, R2, and D, while neighboring nodes of R1 are R2 and D, and the neighboring node of R2 is D. Then, we assumed each broadcast node knows the perfect CSI of communication links between itself and each of its neighboring nodes by pilot broadcasting. Our cooperative network also assumes that S always has the packet to be transmitted. And if the signals with strong enough SNR, which is more than the current threshold, are transmitted to D, S will be set as the next broadcast node to transmit the new signals, and relay nodes clear data cache, which is indicated that one delivery is completed. Additionally,

when transmitting the same packet to the same node, S has the highest transmission priority, R2 has the second priority, and R1 has the lowest priority. This is because S has fixed power support, which does not consider the energy state when transmitting packets. This way can save the harvested energy of relay nodes in order to be used in the case where only relay nodes can transmit the packet. Furthermore, the OR protocol consists of three steps:

1) Determine the TCs  $S(i) \in \{s_1, s_2, s_3, s_4, s_5, s_6\}$  in the current time slot, where  $s_1 = \{S\}$ ,  $s_2 = \{S, R1\}$ ,  $s_3 = \{S, R2\}$ ,  $s_4 = \{(S, R1, R2)_1\}$ ,  $s_5 = \{(S, R1, R2)_2\}$ ,  $s_6 = \{(S, R1, R2)_3\}$ . Especially, the term  $(S, R1, R2)_1$  means the situation of the packet from R1 to R2, when both S and R1 have the packet. Term  $(S, R1, R2)_2$  represents that the packet at R2 is from S, when both S and R1 have the packet. Term  $(S, R1, R2)_3$  represents that S transmits the packet to R1 and R2 in the same slot.

2) On the basis of the CSI between nodes, the stored energy  $B_1(i)$  of R1 and the stored energy  $B_2(i)$  of R2, the transmitter node  $\in \{S, R1, R2, \approx\}$  is selected from the TCs  $S(i)$ , where term  $\approx$  means that all nodes keep silent in the current time slot.

3) Determine the effective transmission and get TCs  $S(i+1) \in \{s_1, s_2, s_3, s_4, s_5, s_6\}$  in the next time slot.

Based on the above rules and the system model assumptions in Section II-A, the following transmission priority of node is proposed to realize the efficient transmission of data packets from S to D:

- When  $TCs(i) = \{S\}$ , S will first consider sending data packets to D, and then consider sending data packets to R1 or R2 if the transmission from S to D fails. If S fails to transmit data packets to D, R1 and R2, S remains silent.

- When  $TCs(i) = \{S, R1\}$ , S and R1 will first consider sending data packets to D, and S has a higher priority than R1. In the case that both S and R1 fail to transmit data packets to D, S and R1 will consider sending data packets to R2, and the priority of S is higher than that of R1. If S and R1 fail to transmit data packets to D and R2 respectively, both S and R1 nodes remain silent.

- When  $TCs(i) = \{S, R2\}$ , S and R2 will consider sending data packets to D, and S has a higher priority than R2. In the case that both S and R2 fail to transmit data packets to D, both S and R2 remain silent.

- When  $TCs(i) = \{S, R1, R2\}$ , S, R1 and R2 will respectively consider sending data packets to D, where S has the highest priority, R2 has the second priority, and R1 has the lowest priority. If S, R2 and R1 fail to transmit data packets to D, S, R2 and R1 remain silent.

Moreover, the above node transmission priority can be generalized as follows:

- When selecting the transmitter candidates for data transmission in the TCs set  $S(i)$ , except for S, the node close to the destination node of data transmission is prioritized as the transmitter candidate.

- When selecting the destination node for data transmission in the non-TC set  $\bar{S}(i)$ , except for D, the node closer to

D is prioritized as the destination node. In particular, once the relay node of a node becomes a TC, this node will no longer be considered as the destination node.

In details, all cases of OR protocol are shown in Table 4. Because of transmitting packets by broadcasting, D can receive all signals of the same packet to combine by MRC even in the different time slot, no matter which the transmitter is. Therefore, we use  $\gamma$  (like  $\gamma_{SD}$ ) without  $(i)$  to represent the SNR of the signal of the same packet received by D in the previous time slot. In addition, all  $\gamma(i)$  (like  $\gamma_{SD}(i)$ ) represent the SNR of the corresponding link in the current time slot. Assume that D received a signal with  $\gamma_1$  SNR and a signal of the same packet with  $\gamma_2$  SNR in the previous time slot. After MRC technique processing, the overall SNR of the signal received by D is  $\gamma_{overall} = \gamma_1 + \gamma_2$ . Hence, to meet the SNR threshold  $\Gamma_{th}$ , each node only needs to transmit the signal with  $\Gamma_{th} - \gamma_{overall}$  SNR, which reduces the need for high-quality channels and improves the performance of the network. For example, when  $TCs(i) = \{S, R1\}$ , the  $\gamma_{overall}$  is  $\gamma_{SD}$  which was received by D when S transmitted the signal to R1 in the previous time slot by broadcasting way. Terms  $\gamma_{overall1}$ ,  $\gamma_{overall2}$  and  $\gamma_{overall3}$  represent the SNR, which has been received by D, when  $TCs(i) = \{S, R1\}$ ,  $TCs(i) = \{S, R2\}$  and  $TCs(i) = \{S, R1, R2\}$  respectively. Obviously,  $\gamma_{overall1}$ ,  $\gamma_{overall2}$  and  $\gamma_{overall3}$  are less than  $\Gamma_{th}$ .

### III. LIMITING DISTRIBUTION OF ENERGY

In this section, the expressions for the limiting distributions of energy in the PEB of R1 and R2, assuming it to be of infinite size, are derived and analyzed. The input harvest energy  $X(i)$  in the  $i$ -th time slot is assumed to be an exponentially distributed random variable with probability density function (PDF)  $f_X(x)$ . With the mean  $\mathbb{E}[X(i)] = 1/\lambda$ , the PDF of  $X(i)$  can be expressed as

$$f_X(x) = \lambda e^{-\lambda x}, \quad x > 0. \quad (10)$$

Obviously, the energy harvesting parameter  $\lambda$  of R1 and R2 are independent. Thus, let  $\lambda_1$  represent the parameter of R1, and  $\lambda_2$  represent the parameter of R2.

In order to clearly describe the theoretical derivation process, letters ‘c’, ‘d’, ‘f’, ‘g’, ‘m’, ‘n’ and ‘o’ are used, whose upper cases represent conditions and lower cases represent corresponding probability values. For example,

$$\mathbb{C} \triangleq \gamma_{overall1} + \gamma_{SD2}(i) < \Gamma_{th}, \quad (11)$$

$$\Pr\{\gamma_{overall1} + \gamma_{SD}(i) < \Gamma_{th}\} = \Pr\{\mathbb{C}\} = c \quad (12)$$

Case- $\mathbb{C}$  means the D node receives a signal from the S node first, but the SNR of the signal is less than the threshold. Furthermore, after some slots, D receives the signal from S again, while after the MRC algorithm combines the signals, the sum of SNR is still less than the threshold. And, obviously,  $\bar{\mathbb{C}}$  means the sum of SNR is greater than or equal to the threshold as well as  $\bar{\mathbb{C}} = 1 - c$ . In Table 5, all alias are shown.

**TABLE 4.** The OR protocol. In the current time slot, the protocol determines the transmitter node and effective transmission according to the known transmitter candidates set  $TCs(i)$  and the known conditions (energy information stored by relay nodes, the current channel information, and the overall SNR of the current packet which has been combined by MRC technique), and further obtains the  $TCs(i+1)$  of the next time slot.

$TCs(i)$	transmitter	effective transmission	conditions	$TCs(i+1)$
S	S	S→D	$\gamma_{SD}(i) \geq \Gamma_{th}$	S
	S	S→R1,R2	$\gamma_{SR1}(i) \geq \Gamma_{th}, \gamma_{SR2}(i) \geq \Gamma_{th}, \gamma_{SD}(i) < \Gamma_{th}$	(S,R1,R2) <sub>3</sub>
	S	S→R2	$\gamma_{SR2}(i) \geq \Gamma_{th}, \gamma_{SR1}(i) < \Gamma_{th}, \gamma_{SD}(i) < \Gamma_{th}$	S,R2
	S	S→R1	$\gamma_{SR1}(i) \geq \Gamma_{th}, \gamma_{SR2}(i) < \Gamma_{th}, \gamma_{SD}(i) < \Gamma_{th}$	S,R1
	≈	≈	others	S
S,R1	S	S→D	$\gamma_{overall1} + \gamma_{SD}(i) \geq \Gamma_{th}$	S
	R1	R1→D	$\gamma_{overall1} + \gamma_{R1D}(i) \geq \Gamma_{th}, B_1(i) \geq M_{R1}, \gamma_{overall1} + \gamma_{SD}(i) < \Gamma_{th}$	S
	S	S→R2	$\gamma_{SR2}(i) \geq \Gamma_{th}, \gamma_{overall1} + \gamma_{R1D}(i) < \Gamma_{th}, B_1(i) \geq M_{R1}, \gamma_{overall1} + \gamma_{SD}(i) < \Gamma_{th}$	(S,R1,R2) <sub>1</sub>
	S	S→R2	$\gamma_{SR2}(i) \geq \Gamma_{th}, B_1(i) < M_{R1}, \gamma_{overall1} + \gamma_{SD}(i) < \Gamma_{th}$	(S,R1,R2) <sub>1</sub>
	R1	R1→R2	$\gamma_{R1R2}(i) \geq \Gamma_{th}, \gamma_{SR2}(i) < \Gamma_{th}, B_1(i) \geq M_{R1}, \gamma_{overall1} + \gamma_{SD}(i) < \Gamma_{th}$	(S,R1,R2) <sub>2</sub>
	≈	≈	others	S,R1
S,R2	S	S→D	$\gamma_{overall2} + \gamma_{SD}(i) \geq \Gamma_{th}$	S
	R2	R2→D	$\gamma_{overall2} + \gamma_{R2D}(i) \geq \Gamma_{th}, \gamma_{overall2} + \gamma_{SD}(i) < \Gamma_{th}$	S
	≈	≈	others	S,R2
(S,R1,R2) <sub>1</sub>	S	S→D	$\gamma_{overall3} + \gamma_{SD2}(i) \geq \Gamma_{th}, B_2(i) \geq M_{R2}$	S
	R1	R1→D	$\gamma_{overall3} + \gamma_{R1D}(i) \geq \Gamma_{th}, \gamma_{overall3} + \gamma_{R2D}(i) < \Gamma_{th}, \gamma_{overall3} + \gamma_{SD}(i) < \Gamma_{th}, B_1(i) \geq M_{R1}$	S
	R2	R2→D	$\gamma_{SD} + \gamma_{R1D} + \gamma_{R2D}(i) \geq \Gamma_{th}, \gamma_{overall3} + \gamma_{SD}(i) < \Gamma_{th}, B_2(i) \geq M_{R2}$	S
	≈	≈	others	(S,R1,R2) <sub>1</sub>
(S,R1,R2) <sub>2</sub>	S	S→D	$\gamma_{overall3} + \gamma_{SD}(i) \geq \Gamma_{th}$	S
	R1	R1→D	$\gamma_{overall3} + \gamma_{R1D}(i) \geq \Gamma_{th}, \gamma_{overall3} + \gamma_{R2D}(i) \geq \Gamma_{th}, \gamma_{overall3} + \gamma_{SD}(i) < \Gamma_{th}$	S
	R2	R2→D	$\gamma_{overall3} + \gamma_{R2D}(i) \geq \Gamma_{th}, \gamma_{overall3} + \gamma_{SD}(i) < \Gamma_{th}$	S
	≈	≈	others	(S,R1,R2) <sub>2</sub>
(S,R1,R2) <sub>3</sub>	S	S→D	$\gamma_{overall3} + \gamma_{SD}(i) \geq \Gamma_{th}$	S
	R1	R1→D	$\gamma_{overall3} + \gamma_{R1D}(i) \geq \Gamma_{th}, \gamma_{overall3} + \gamma_{R2D}(i) < \Gamma_{th}, \gamma_{overall3} + \gamma_{SD}(i) < \Gamma_{th}$	S
	R2	R2→D	$\gamma_{overall3} + \gamma_{R2D}(i) \geq \Gamma_{th}, \gamma_{overall3} + \gamma_{SD}(i) < \Gamma_{th}$	S
	≈	≈	others	(S,R1,R2) <sub>3</sub>

Then, we can similarly get

$$\mathbb{D} \triangleq \gamma_{overall1} + \gamma_{R1D}(i) < \Gamma_{th}, \quad (13)$$

$$\mathbb{F} \triangleq \gamma_{overall3} + \gamma_{R2D}(i) < \Gamma_{th}, \quad (14)$$

$$\mathbb{G} \triangleq \gamma_{overall3} + \gamma_{R1D2}(i) < \Gamma_{th}, \quad (15)$$

$$\mathbb{M} \triangleq \gamma_{overall2} + \gamma_{R2D}(i) < \Gamma_{th}, \quad (16)$$

$$\mathbb{N} \triangleq \gamma_{overall2} + \gamma_{R2D}(i) < \Gamma_{th}, \quad (17)$$

$$\mathbb{O} \triangleq \gamma_{overall3} + \gamma_{SD2}(i) < \Gamma_{th}, \quad (18)$$

To obtain the expressions for PDF of energy in the PEB of R1 and R2, the probability of the transmitter candidate state needs to be calculated in advance. In [19], we know, by using the state transition matrix (STM)  $T$  of two adjacent time slots, each transmitter candidate state occurrence probabilities,  $p_s = \Pr\{TCs = \{S\}\}$ ,  $p_{SR1} = \Pr\{TCs = \{S, R1\}\}$ ,  $p_{SR2} = \Pr\{TCs = \{S, R2\}\}$ ,  $p_1 = \Pr\{P1\}$ ,  $p_2 = \Pr\{P2\}$  and  $p_3 = \Pr\{P3\}$ , can be updated iteratively until they converge to get their theoretical value, where  $P1$

represents (S,R1,R2)<sub>1</sub>,  $P2$  represents (S,R1,R2)<sub>2</sub>,  $P3$  represents (S,R1,R2)<sub>3</sub>. Obviously,  $p_1 + p_2 + p_3 = p_{SR1R2} = \Pr\{TCs = \{S, R1, R2\}\}$ . And the STM  $T$  can be constructed as follows (19) as shown at the bottom of the next page, where the element  $p_{i-j}(i, j \in \{S, SR1, SR2, (SR1R2)_1, (SR1R2)_2, (SR1R2)_3\})$  represents the probability that the transmitter candidate state changes from state  $i$  at the current time slot to state  $j$  at the next time slot, satisfying  $\sum_{j \in \{S, SR1, SR2, (SR1R2)_1, (SR1R2)_2, (SR1R2)_3\}} p_{i-j} = 1$ . The details of the algorithm for the STM-based theoretical solutions of the transmitter candidate state probability can be seen in [19]. According to the OR protocol introduced in Section II, we have

$$\begin{aligned} p_{S-S} &= \Pr\{\gamma_{SD}(i) < \Gamma_{th}, \gamma_{SR2}(i) < \Gamma_{th}, \gamma_{SR1}(i) < \Gamma_{th}\} \\ &\quad + \Pr\{\gamma_{SD}(i) \geq \Gamma_{th}\} \\ &= \left(1 - e^{-W_{SD}\Gamma_{th}}\right) \left(1 - e^{-W_{SR2}\Gamma_{th}}\right) \left(1 - e^{-W_{SR1}\Gamma_{th}}\right) \\ &\quad + e^{-W_{SD}\Gamma_{th}}, \end{aligned} \quad (20)$$

TABLE 5. All failure transmission case only considering CSI in system table.

TCs(I)	transmitter	receiver	condition	alias
S	S	D	$\gamma_{SD}(i) < \Gamma_{th}$	A
	S	R1,R2	$\gamma_{SR1}(i) < \Gamma_{th}, \gamma_{SR2}(i) < \Gamma_{th}$	B
	S	R2	$\gamma_{SR2}(i) < \Gamma_{th}$	Q
	S	R1	$\gamma_{SR1}(i) < \Gamma_{th}$	R
S,R1	S	D	$\gamma_{overall1} + \gamma_{SD}(i) < \Gamma_{th}$	C
	R1	D	$\gamma_{overall1} + \gamma_{R1D}(i) < \Gamma_{th}$	D
	S	R2	$\gamma_{SR2} < \Gamma_{th}$	S
	R1	R2	$\gamma_{R1R2} < \Gamma_{th}$	T
S,R2	S	D	$\gamma_{overall2} + \gamma_{SD}(i) < \Gamma_{th} < \Gamma_{th}$	M
	R2	D	$\gamma_{overall2} + \gamma_{R2D}(i) < \Gamma_{th}$	N
(S,R1,R2) <sub>1</sub>	S	D	$\gamma_{overall3} + \gamma_{SD}(i) < \Gamma_{th}$	O
	R1	D	$\gamma_{overall3} + \gamma_{R1D}(i) < \Gamma_{th}$	G
	R2	D	$\gamma_{overall3} + \gamma_{R2D}(i) < \Gamma_{th}$	F
(S,R1,R2) <sub>2</sub>	S	D	$\gamma_{overall3} + \gamma_{SD}(i) < \Gamma_{th}$	O
	R1	D	$\gamma_{overall3} + \gamma_{R1D}(i) < \Gamma_{th}$	G
	R2	D	$\gamma_{overall3} + \gamma_{R2D}(i) < \Gamma_{th}$	F
(S,R1,R2) <sub>3</sub>	S	D	$\gamma_{overall3} + \gamma_{SD}(i) < \Gamma_{th}$	O
	R1	D	$\gamma_{overall3} + \gamma_{R1D}(i) < \Gamma_{th}$	G
	R2	D	$\gamma_{overall3} + \gamma_{R2D}(i) < \Gamma_{th}$	F

$$p_{S-SR1} = \Pr\{\gamma_{SD}(i) < \Gamma_{th}, \gamma_{SR2}(i) < \Gamma_{th}, \gamma_{SR1}(i) \geq \Gamma_{th}\} = (1 - e^{-W_{SD}\Gamma_{th}})(1 - e^{-W_{SR2}\Gamma_{th}})e^{-W_{SR1}\Gamma_{th}}, \quad (21)$$

$$p_{S-SR2} = \Pr\{\gamma_{SD}(i) < \Gamma_{th}, \gamma_{SR1}(i) < \Gamma_{th}, \gamma_{SR2}(i) \geq \Gamma_{th}\} = (1 - e^{-W_{SD}\Gamma_{th}})(1 - e^{-W_{R1D}\Gamma_{th}})e^{-W_{SR2}\Gamma_{th}}, \quad (22)$$

$$p_{S-(SR1R2)_3} = \Pr\{\gamma_{SD}(i) < \Gamma_{th}, \gamma_{SR1}(i) \geq \Gamma_{th}, \gamma_{SR2}(i) \geq \Gamma_{th}\} = (1 - e^{-W_{SD}\Gamma_{th}})e^{-W_{R1D}\Gamma_{th}}e^{-W_{SR2}\Gamma_{th}}, \quad (23)$$

$$p_{SR1-S} = \Pr\{\bar{C}\} + \Pr\{B_1(i) \geq M_{R1}, C, \bar{D}\} = (1 - c) + c * PU1 * (1 - d), \quad (24)$$

$$p_{SR1-(SR1R2)_1} = \Pr\{C, B_1(i) \geq M_{R1}, D, \gamma_{R1R2}(i) \geq \Gamma_{th}, \gamma_{SR2}(i) \geq \Gamma_{th}\} = c * PU1 * d * e^{-W_{R1R2}\Gamma_{th}} * (1 - W_{SR2}\Gamma_{th}), \quad (25)$$

$$p_{SR1-(SR1R2)_2} = \Pr\{C, B_1(i) \geq M_{R1}, D, \gamma_{SR2}(i) \geq \Gamma_{th}\} + \Pr\{C, B_1(i) < M_{R1}, \gamma_{R1R2}(i) \geq \Gamma_{th}\} = c * PU1 * d * e^{-W_{SR2}\Gamma_{th}} + c * (1 - PU1) * e^{-W_{SR2}\Gamma_{th}}, \quad (26)$$

$$p_{SR1-SR1} = 1 - p_{SR1-(SR1R2)_1} - p_{SR1-S} - p_{SR1-(SR1R2)_2}, \quad (27)$$

$$p_{SR2-S} = \Pr\{\bar{M}\} + \Pr\{B_2(i) \geq M_{R2}, M, \bar{N}\} = (1 - m) + PU2 * m * (1 - n), \quad (28)$$

$$p_{SR2-SR2} = \Pr\{B_2(i) \geq M_{R2}, M, N\} + \Pr\{B_2(i) < M_{R2}\} = 1 - p_{SR2-S}, \quad (29)$$

$$p_{(SR1R2)_1-S} = (1 - o) + o * (PU2 * (1 - f) + (PU2 * f + (1 - PU2)) * PU1 * (1 - g)), \quad (30)$$

$$p_{(SR1R2)_1-(SR1R2)_1} = 1 - p_{(SR1R2)_1-S}, \quad (31)$$

$$p_{(SR1R2)_2-S} = (1 - o) + o * (PU2 * (1 - f) + (PU2 * f + (1 - PU2)) * PU1 * (1 - g)), \quad (32)$$

$$p_{(SR1R2)_2-(SR1R2)_2} = 1 - p_{(SR1R2)_2-S}, \quad (33)$$

$$p_{(SR1R2)_3-S} = (1 - o) + o * (PU2 * (1 - f) + (PU2 * f + (1 - PU2)) * PU1 * (1 - g)), \quad (34)$$

$$p_{(SR1R2)_3-(SR1R2)_3} = 1 - p_{(SR1R2)_3-S}, \quad (35)$$

where,  $PU1 = \frac{1}{b_1 \lambda_1 M_{R1}}$  and  $PU2 = \frac{1}{b_2 \lambda_2 M_{R2}}$ .  $b_1$  and  $b_2$  are given in (65) and (58). And the proof of  $PU1$  and  $PU2$  are given in (75) and (77). And the remaining elements of  $T$  are equal to 0.

In order to get  $T$ , the values of ‘c’, ‘d’, ‘f’, ‘g’, ‘m’, ‘n’ and ‘o’ are required. Before this step, it is foundation to get the probability distributions  $p_{\gamma_{overall1}}(j)$ ,  $p_{\gamma_{overall2}}(j)$ ,  $p_{\gamma_{overall3}}(j)$  of  $\gamma_{overall1}$ ,  $\gamma_{overall2}$  and  $\gamma_{overall3}$ . For example,  $p_{\gamma_{overall1}}(j)$  is the probability that node D has received the SNR of value  $(\frac{j-1}{N}\Gamma_{th} \leq \gamma_{overall1} < \frac{j}{N}\Gamma_{th})$  when TCs = {S, R1}. To obtain these probability distributions, the STM method is used. STM  $T1$ , STM  $T2$  and STM  $T3$  correspond to  $p_{\gamma_{overall1}}$ ,  $p_{\gamma_{overall2}}$  and  $p_{\gamma_{overall3}}$  respectively. The size of  $T1$  is  $N \times N$  dimension. The states of  $T1$  are the value of  $\gamma_{overall1}$  and the element  $T1(i, j)$  means the transition probability from  $(\frac{i-1}{N}\Gamma_{th} \leq \gamma_{overall1} < \frac{i}{N}\Gamma_{th})$  to  $(\frac{j-1}{N}\Gamma_{th} \leq \gamma_{overall1} < \frac{j}{N}\Gamma_{th})$ , where  $1 \leq i, j \leq N$  and  $i, j \in Z$ . The elements of  $T1$  are as follows:

$$T1(i, j) = \left( 1 - \int_0^{\frac{N-i}{N}\Gamma_{th}} f_{SD}(x) dx \times \left( PU1 \int_0^{\frac{N-i}{N}\Gamma_{th}} f_{R1D}(x) dx \times \int_0^{\Gamma_{th}} f_{SR2}(x) dx \int_0^{\Gamma_{th}} f_{R1R2}(x) dx + (1 - PU1) \int_0^{\Gamma_{th}} f_{SR2}(x) dx \right) \right) \times \int_{\frac{i-1}{N}\Gamma_{th}}^{\frac{j}{N}\Gamma_{th}} f_{SD}(x) dx / \int_0^{\Gamma_{th}} f_{SD}(x) dx \quad i \neq j \quad (36)$$

$$T = \begin{bmatrix} p_{S-S} & p_{S-SR1} & p_{S-SR2} & p_{S-(SR1R2)_1} & p_{S-(SR1R2)_2} & p_{S-(SR1R2)_3} \\ p_{SR1-S} & p_{SR1-SR1} & p_{SR1-SR2} & p_{SR1-(SR1R2)_1} & p_{SR1-(SR1R2)_2} & p_{SR1-(SR1R2)_3} \\ p_{SR2-S} & p_{SR2-SR1} & p_{SR2-SR2} & p_{SR2-(SR1R2)_1} & p_{SR2-(SR1R2)_2} & p_{SR2-(SR1R2)_3} \\ p_{(SR1R2)_1-S} & p_{(SR1R2)_1-SR1} & p_{(SR1R2)_1-SR2} & p_{(SR1R2)_1-(SR1R2)_1} & p_{(SR1R2)_1-(SR1R2)_2} & p_{(SR1R2)_1-(SR1R2)_3} \\ p_{(SR1R2)_2-S} & p_{(SR1R2)_2-SR1} & p_{(SR1R2)_2-SR2} & p_{(SR1R2)_2-(SR1R2)_1} & p_{(SR1R2)_2-(SR1R2)_2} & p_{(SR1R2)_2-(SR1R2)_3} \\ p_{(SR1R2)_3-S} & p_{(SR1R2)_3-SR1} & p_{(SR1R2)_3-SR2} & p_{(SR1R2)_3-(SR1R2)_1} & p_{(SR1R2)_3-(SR1R2)_2} & p_{(SR1R2)_3-(SR1R2)_3} \end{bmatrix} \quad (19)$$

$$\begin{aligned}
 T1(i, j) = & \left( 1 - \int_0^{\frac{N-i}{N}\Gamma_{th}} f_{SD}(x) dx \right. \\
 & \times \left( PU1 \int_0^{\frac{N-i}{N}\Gamma_{th}} f_{R1D}(x) dx \right. \\
 & \times \int_0^{\Gamma_{th}} f_{SR2}(x) dx \int_0^{\Gamma_{th}} f_{R1R2}(x) dx \\
 & \left. \left. + (1 - PU1) \int_0^{\Gamma_{th}} f_{SR2}(x) dx \right) \right) \\
 & \times \int_{\frac{i-1}{N}\Gamma_{th}}^{\frac{j}{N}\Gamma_{th}} f_{SD}(x) dx / \int_0^{\Gamma_{th}} f_{SD}(x) dx \\
 & + \int_0^{\frac{N-i}{N}\Gamma_{th}} f_{SD}(x) dx \\
 & \times \left( PU1 \int_0^{\frac{N-i}{N}\Gamma_{th}} f_{R1D}(x) dx \right. \\
 & \times \int_0^{\Gamma_{th}} f_{SR2}(x) dx \int_0^{\Gamma_{th}} f_{R1R2}(x) dx \\
 & \left. + (1 - PU1) \int_0^{\Gamma_{th}} f_{SR2}(x) dx \right) \\
 & i = j \tag{37}
 \end{aligned}$$

Similarly, the elements of  $T2$  and  $T3$  are as follows:

$$\begin{aligned}
 T2(i, j) = & \left( 1 - \int_0^{\frac{N-i}{N}\Gamma_{th}} f_{SD}(x) dx \right. \\
 & \times \left( PU2 \int_0^{\frac{N-i}{N}\Gamma_{th}} f_{R2D}(x) dx + (1 - PU2) \right) \\
 & \times \int_{\frac{i-1}{N}\Gamma_{th}}^{\frac{j}{N}\Gamma_{th}} f_{SD}(x) dx / \int_0^{\Gamma_{th}} f_{SD}(x) dx \\
 & i \neq j \tag{38}
 \end{aligned}$$

$$\begin{aligned}
 T2(i, j) = & \left( 1 - \int_0^{\frac{N-i}{N}\Gamma_{th}} f_{SD}(x) dx \right. \\
 & \times \left( PU2 \int_0^{\frac{N-i}{N}\Gamma_{th}} f_{R2D}(x) dx + (1 - PU2) \right) \\
 & \times \int_{\frac{i-1}{N}\Gamma_{th}}^{\frac{j}{N}\Gamma_{th}} f_{SD}(x) dx / \int_0^{\Gamma_{th}} f_{SD}(x) dx \\
 & + \int_0^{\frac{N-i}{N}\Gamma_{th}} f_{SD}(x) dx \\
 & \times \left( PU2 \int_0^{\frac{N-i}{N}\Gamma_{th}} f_{R2D}(x) dx + (1 - PU2) \right) \\
 & i = j \tag{39}
 \end{aligned}$$

$$\begin{aligned}
 T3(i, j) = & \left( 1 - \int_0^{\frac{N-i}{N}\Gamma_{th}} f_{SD}(x) dx \right. \\
 & \times \left( PU2 \int_0^{\frac{N-i}{N}\Gamma_{th}} f_{R2D}(x) dx + (1 - PU2) \right) \\
 & \times \left( PU1 \int_0^{\frac{N-i}{N}\Gamma_{th}} f_{R1D}(x) dx + (1 - PU1) \right)
 \end{aligned}$$

$$\begin{aligned}
 T3(i, j) = & \left( 1 - \int_0^{\frac{N-i}{N}\Gamma_{th}} f_{SD}(x) dx \right. \\
 & \times \left( PU2 \int_0^{\frac{N-i}{N}\Gamma_{th}} f_{R2D}(x) dx + (1 - PU2) \right) \\
 & \times \left( PU1 \int_0^{\frac{N-i}{N}\Gamma_{th}} f_{R1D}(x) dx + (1 - PU1) \right) \\
 & i \neq j \\
 & \times \left( \frac{p_3}{p_1 + p_2 + p_3} \frac{\int_{\frac{i-1}{N}\Gamma_{th}}^{\frac{j}{N}\Gamma_{th}} f_{SD}(x) dx}{\int_0^{\Gamma_{th}} f_{SD}(x) dx} \right. \\
 & + \frac{p_2}{p_1 + p_2 + p_3} \frac{p_{d_{S \rightarrow R2}}(j)}{\sum_{k=1}^N p_{d_{S \rightarrow R2}}(k)} \\
 & + \frac{p_1}{p_1 + p_2 + p_3} \frac{p_{d_{R1 \rightarrow R2}}(j)}{\sum_{k=1}^N p_{d_{R1 \rightarrow R2}}(k)} \\
 & \left. + \int_0^{\frac{N-i}{N}\Gamma_{th}} f_{SD}(x) dx \right) \\
 & \times \left( PU2 \int_0^{\frac{N-i}{N}\Gamma_{th}} f_{R2D}(x) dx + (1 - PU2) \right) \\
 & \times \left( PU1 \int_0^{\frac{N-i}{N}\Gamma_{th}} f_{R1D}(x) dx + (1 - PU1) \right) \\
 & i = j \tag{40}
 \end{aligned}$$

where  $p_{d_{S \rightarrow R2}}(j)$  is the probability that node D receives the SNR of value  $(\frac{i-1}{N}\Gamma_{th} \leq \gamma_{overall1} + \gamma_{SD} < \frac{j}{N}\Gamma_{th})$  when system has transitioned the TCs state from  $\{S, R1\}$  to  $\{S, R1, R2\}_1$ , while  $p_{d_{R1 \rightarrow R2}}(j)$  is the probability that node D receives the SNR of value  $(\frac{i-1}{N}\Gamma_{th} \leq \gamma_{overall1} + \gamma_{R1D} < \frac{j}{N}\Gamma_{th})$  when system has transitioned the TCs state from  $\{S, R1\}$  to  $\{S, R1, R2\}_2$ . Obviously, the expressions of  $p_{d_{S \rightarrow R2}}(j)$  and  $p_{d_{R1 \rightarrow R2}}(j)$  are as follows:

$$p_{d_{S \rightarrow R2}}(j) = \text{conv}(p_{\gamma_{overall1}}, p_{SD}) \tag{42}$$

$$p_{d_{R1 \rightarrow R2}}(j) = \text{conv}(p_{\gamma_{overall1}}, p_{R1D}) \tag{43}$$

where

$$p_{SD}(j) = \int_{\frac{i-1}{N}\Gamma_{th}}^{\frac{j}{N}\Gamma_{th}} f_{SD}(x) dx \tag{44}$$

$$p_{R1D}(j) = \int_{\frac{i-1}{N}\Gamma_{th}}^{\frac{j}{N}\Gamma_{th}} f_{R1D}(x) dx. \tag{45}$$



Similarly,

$$p_{R2D}(j) = \int_{\frac{j-1}{N}\Gamma_{th}}^{\frac{j}{N}\Gamma_{th}} f_{R2D}(x) dx. \quad (46)$$

With these parameter, the expressions of ‘c’, ‘d’, ‘f’, ‘g’, ‘m’, ‘n’ and ‘o’ can be derived.

$$c = \sum_{j=1}^N \text{conv}(p_{\gamma_{overall1}}, PSD) \quad (47)$$

$$d = \sum_{j=1}^N \text{conv}(p_{\gamma_{overall1}}, PR1D) \quad (48)$$

$$m = \sum_{j=1}^N \text{conv}(p_{\gamma_{overall2}}, PSD) \quad (49)$$

$$n = \sum_{j=1}^N \text{conv}(p_{\gamma_{overall2}}, PR2D) \quad (50)$$

$$f = \sum_{j=1}^N \text{conv}(p_{\gamma_{overall3}}, PR2D) \quad (51)$$

$$g = \sum_{j=1}^N \text{conv}(p_{\gamma_{overall3}}, PR1D) \quad (52)$$

$$o = \sum_{j=1}^N \text{conv}(p_{\gamma_{overall3}}, PSD) \quad (53)$$

The detailed process for obtaining probability  $p_s$ ,  $p_{SR1}$ ,  $p_{SR2}$ ,  $p_1$ ,  $p_2$ ,  $p_3$ ,  $p_{\gamma_{overall1}}(j)$ ,  $p_{\gamma_{overall2}}(j)$ ,  $p_{\gamma_{overall3}}(j)$ , ‘c’, ‘d’, ‘f’, ‘g’, ‘m’, ‘n’ and ‘o’ is shown in Alg. 1. See Appendix A.

As the preparations are ready, in Sections III-A and III-B, the PDF of energy in the PEB of R1 and R2 are obtained, respectively.

### A. LIMITING DISTRIBUTION OF R2 ENERGY

By using the DCSMC and donating the energy level in the infinite-size energy buffer in the  $i$ -th signaling interval as  $B_2(i)$ , the PEB’s buffer of R2 update equations are given by

$$\begin{aligned} B_2(i+1) &= B_2(i) + X(i), & \mathbb{P}_{21} \\ B_2(i+1) &= B_2(i) - M_{R2} + X(i), & \mathbb{P}_{22} \end{aligned} \quad (54)$$

where  $\mathbb{P}_{21}$  and  $\mathbb{P}_{22}$  are the applicable conditions of the update equations, respectively. They are given by

$$\begin{aligned} \mathbb{P}_{21} : & (TCs = \{S\}) \cup (TCs = \{S, R1\}) \\ & \cup [(TCs = \{S, R2\}) \cap (B_2(i) < M_{R2})] \\ & \cup [(TCs = \{S, R2\}) \cap (B_2(i) \geq M_{R2}) \cap \mathbb{M} \cap \mathbb{N}] \\ & \cup [(TCs = \{S, R2\}) \cap (B_2(i) \geq M_{R2}) \cap \overline{\mathbb{M}}] \\ & \cup [(TCs = \{S, R1, R2\}) \cap (B_2(i) \geq M_{R2} \cap \mathbb{O} \cap \mathbb{F})] \\ & \cup [(TCs = \{S, R1, R2\}) \cap (B_2(i) \geq M_{R2} \cap \overline{\mathbb{O}})] \end{aligned}$$

$$\cup [(TCs = \{S, R1, R2\}) \cap (B_2(i) < M_{R2})], \quad (55)$$

$$\begin{aligned} \mathbb{P}_{22} : & [(TCs = \{S, R2\}) \cap (B_2(i) \geq M_{R2}) \cap \mathbb{C} \cap \overline{\mathbb{N}}] \\ & \cup [(TCs = \{S, R1, R2\}) \cap (B_2(i) \geq M_{R2} \cap \mathbb{O} \cap \overline{\mathbb{F}})]. \end{aligned} \quad (56)$$

Let  $\psi_{R2}$  represents the energy buffer convergence parameter for the energy update process  $B_1(i)$  of Eq. (54), with the help of the Eq. (47) to Eq. (53), which can be expressed as follows

$$\begin{aligned} \psi_{R2} &= \lambda_2 M_{R2} [p_{SR2} * m(1-n) + (p_1 + p_2 + p_3) * o(1-f)] \\ &= \lambda_2 M_{R2} b_2, \end{aligned} \quad (57)$$

where

$$b_2 = p_{SR2} * m(1-n) + (p_1 + p_2 + p_3) * o(1-f). \quad (58)$$

The limiting PDF when  $\psi_{R2} > 1$  is obtained in Theorem 1, and the scenario when  $\psi_{R2} \leq 1$  is discussed in Theorem 2.

*Theorem 1:* If  $\psi_{R2} > 1$ , the energy update process  $B_2(i)$  in Eq. (54) will have a stationary distribution. Furthermore, the limiting PDF of the energy buffer state at R2 can be expressed by

$$g_2(x) = \begin{cases} \frac{1}{M_{R2}}(1 - e^{Q_2 x}), & 0 \leq x < M_{R2} \\ \frac{1}{M_{R2}} \frac{-Q_2 e^{Q_2 x}}{(b_2 \lambda_2 + Q_2)}, & x \geq M_{R2}. \end{cases} \quad (59)$$

where

$$Q_2 = \frac{-W(-b_2 \lambda_2 M_{R2} e^{-b_2 \lambda_2 M_{R2}})}{M_{R2}} - b_2 \lambda_2 < 0, \quad (60)$$

satisfying  $b_2 \lambda_2 e^{Q_2 M_{R2}} = b_2 \lambda_2 + Q_2$ .

*Proof:* The proof is given in Appendix B. ■

*Theorem 2:* When  $\psi_{R2} \leq 1$ , there is no stationary PDF of the energy buffer state of R1. In addition, after a finite number of time slots, the R1 energy buffer will keep  $B_2(i) > M_{R2}$ .

*Proof:* The proof is given in Appendix C. ■

### B. LIMITING DISTRIBUTION OF R1 ENERGY

Similar to the solution of the limiting distribution of R2 energy, by using the DCSMC and donating the energy level in the infinite-size energy buffer in the  $i$ -th signaling interval as  $B_1(i)$ , the PEB’s buffer of R1 update equations are given by

$$\begin{aligned} B_1(i+1) &= B_1(i) + X(i), & \mathbb{P}_{11} \\ B_1(i+1) &= B_1(i) - M_{R1} + X(i), & \mathbb{P}_{12} \end{aligned} \quad (61)$$

where  $\mathbb{P}_{11}$  and  $\mathbb{P}_{12}$  are the update conditions needed for the equations in Eq. (61) according to OR protocol. Correspondingly, they can be expressed as follows

$$\begin{aligned} \mathbb{P}_{12} : & [(TCs = \{S, R1\}) \cap (B_1(i) \geq M_{R1}) \cap \mathbb{C} \cap \overline{\mathbb{D}}] \\ & \cup [(TCs = \{S, R1\}) \cap ((B_1(i) \geq M_{R1}), \mathbb{C}, \mathbb{D}, \\ & \quad \gamma_{SR2}(i) < \Gamma_{th}, \gamma_{R1R2}(i) \geq \Gamma_{th})] \end{aligned}$$

$$\begin{aligned}
 & \cup \left[ (TCs = \{S, R1, R2\}) \cap (B_2(i) \geq M_{R2}, \mathbb{O}, \mathbb{F}, \right. \\
 & \quad \left. (B_1(i) \geq M_{R1}), \overline{\mathbb{G}} \right] \\
 & \cup \left[ (TCs = \{S, R1, R2\}) \cap (B_2(i) < M_{R2}, \mathbb{O}, \right. \\
 & \quad \left. (B_1(i) \geq M_{R1}), \overline{\mathbb{G}} \right], \quad (62) \\
 \mathbb{P}_{11} : & (TCs = \{S\}) \cup (TCs = \{S, R2\}) \\
 & \cup \left[ (TCs = \{S, R1\}) \cap (B_1(i) < M_{R1}) \right] \\
 & \cup \left[ (TCs = \{S, R1\}) \cap (B_1(i) \geq M_{R1}, \mathbb{C}, \mathbb{D}, \right. \\
 & \quad \left. \gamma_{SR2}(i) \geq \Gamma_{th}, \right) \right] \\
 & \cup \left[ (TCs = \{S, R1\}) \cap (B_1(i) \geq M_{R1}, \mathbb{C}, \mathbb{D}, \right. \\
 & \quad \left. \gamma_{SR2}(i) < \Gamma_{th}, \gamma_{R1R2}(i) < \Gamma_{th}) \right] \\
 & \cup \left[ (P1) \cap (B_2(i) \geq M_{R2}, \mathbb{O}, \overline{\mathbb{F}}) \right] \\
 & \cup \left[ (TCs = \{S, R1, R2\}) \cap (B_2(i) \geq M_{R2}, \mathbb{O}, \mathbb{F}, \right. \\
 & \quad \left. B_1(i) \geq M_{R1}, \mathbb{G}) \right] \\
 & \cup \left[ (TCs = \{S, R1, R2\}) \cap (B_2(i) \geq M_{R2}, \mathbb{O}, \mathbb{F}, \right. \\
 & \quad \left. B_1(i) < M_{R1}) \right] \\
 & \cup \left[ (TCs = \{S, R1, R2\}) \cap (B_2(i) < M_{R2}, \mathbb{O}, \right. \\
 & \quad \left. B_1(i) \geq M_{R1}, \mathbb{G}) \right] \\
 & \cup \left[ (TCs = \{S, R1, R2\}) \cap (B_2(i) < M_{R2}, \mathbb{O}, \right. \\
 & \quad \left. B_1(i) < M_{R1}) \right]. \quad (63)
 \end{aligned}$$

Let  $\psi_{R1}$  represent the energy buffer convergence parameter for the energy update process  $B_1(i)$  of Eq. (61), which can be expressed as follows

$$\begin{aligned}
 \psi_{R1} &= \lambda_1 M_{R1} \left[ p_{SR1} * c \left( (1 - \mathfrak{d}) + \mathfrak{d} \left( 1 - e^{-W_{SR2} \Gamma_{th}} \right) e^{-W_{R1R2} \Gamma_{th}} \right. \right. \\
 & \quad \left. \left. + PU2 \left( (p_1 + p_2 + p_3) * \mathfrak{o} * f(1 - \mathfrak{g}) \right) \right. \right. \\
 & \quad \left. \left. + (1 - PU2) * \left( (p_1 + p_2 + p_3) * \mathfrak{o} (1 - \mathfrak{g}) \right) \right) \right] \\
 &= \lambda_1 M_{R1} b_1, \quad (64)
 \end{aligned}$$

where

$$\begin{aligned}
 b_1 &= p_{SR1} * c \left( (1 - \mathfrak{d}) + \mathfrak{d} \left( 1 - e^{-W_{SR2} \Gamma_{th}} \right) e^{-W_{R1R2} \Gamma_{th}} \right. \\
 & \quad \left. + PU2 \left( (p_1 + p_2 + p_3) * \mathfrak{o} * f(1 - \mathfrak{g}) \right) \right. \\
 & \quad \left. + (1 - PU2) * \left( (p_1 + p_2 + p_3) * \mathfrak{o} (1 - \mathfrak{g}) \right) \right). \quad (65)
 \end{aligned}$$

The limiting PDF when  $\psi_{R1} > 1$  is obtained in Theorem 3, and the scenario when  $\psi_{R1} \leq 1$  is discussed in Theorem 4.

*Theorem 3:* If  $\psi_1 > 1$ , the energy update process  $B_1(i)$  in Eq. (61) will have a stationary distribution. Furthermore,

the limiting PDF of the energy buffer state at R1 can be expressed by

$$g_1(x) = \begin{cases} \frac{1}{M_{R1}} (1 - e^{Q_1 x}), & 0 \leq x < M_{R1} \\ \frac{1}{M_{R1}} \frac{-Q_1 e^{Q_1 x}}{(b_1 \lambda_1 + Q_1)}, & x \geq M_{R1}. \end{cases} \quad (66)$$

And

$$Q_1 = \frac{-W(-b_1 \lambda_1 M_{R1} e^{-b_1 \lambda_1 M_{R1}})}{M_{R1}} - b_1 \lambda_1 < 0, \quad (67)$$

satisfying  $b_1 \lambda_1 e^{Q_1 M_{R1}} = b_1 \lambda_1 + Q_1$ .

*Proof:* The proof is given in Appendix D. ■

*Theorem 4:* Similar to Theorem 2, when  $\psi_{R1} \leq 1$ , there is no stationary PDF of the energy buffer state of R1. And the energy in the R1 energy buffer keeps more than  $M_{R1}$ .

#### IV. ANALYSIS OF OUTAGE PROBABILITY AND THROUGHPUT

This section focuses on the analysis of outage probability, time slot cost, and throughput of our system, when both  $B_1(i)$  and  $B_2(i)$  have limiting PDFs.

According to OR protocol, when all the transmitter candidates fail to transmit signals to the D node, the communication network system is defined as an outage. In an outage, transmitter candidates can transmit the signal to other nodes. Obviously, the system outage probability (OP) can be expressed as

$$OP = r_{pS} + r_{pSR1} + r_{pSR2} + r_{pSR1R2}, \quad (68)$$

where,  $r_{pS}$ ,  $r_{pSR1}$ ,  $r_{pSR2}$  and  $r_{pSR1R2}$  are the outage probability of transmitter candidates set  $\{S\}$ ,  $\{S,R1\}$ ,  $\{SR2\}$ ,  $\{S,R1,R2\}$ , respectively. The outage probability of the node means the transmitter candidates as the broadcast node fail to transmit signals to the D node. Specifically, they can be expressed by

$$\begin{aligned}
 r_{pS} &= p_S \Pr\{\gamma_{SD}(i) < \Gamma_{th}\} \\
 &= p_S \left( 1 - e^{-W_{SD} \Gamma_{th}} \right), \quad (69)
 \end{aligned}$$

$$\begin{aligned}
 r_{pSR1} &= p_{SR1} [\Pr\{\mathbb{C}, \mathbb{D}, B_1(i) \geq M_{R1}\} \\
 & \quad + \Pr\{\mathbb{C}, B_1(i) < M_{R1}\}] \\
 &= p_{SR1} * c (\mathfrak{d} * PU1 + 1 - PU1), \quad (70)
 \end{aligned}$$

$$\begin{aligned}
 r_{pSR2} &= p_{SR2} [\Pr\{\mathbb{M}, \mathbb{N}, B_2(i) \geq M_{R2}\} \\
 & \quad + \Pr\{\mathbb{M}, B_2(i) < M_{R2}\}] \\
 &= p_{SR2} * m (n * PU2 + 1 - PU2), \quad (71)
 \end{aligned}$$

$$\begin{aligned}
 r_{pSR1R2} &= (p_1 + p_2 + p_3) \left[ \Pr\{\mathbb{O}, \mathbb{F}, B_2(i) \geq M_{R2}, \mathbb{G}, B_1(i) \geq M_{R1}\} \right. \\
 & \quad \left. + \Pr\{\mathbb{O}, \mathbb{F}, B_2(i) \geq M_{R2}, B_1(i) < M_{R1}\} \right. \\
 & \quad \left. + \Pr\{\mathbb{O}, B_2(i) < M_{R2}, \mathbb{G}, B_1(i) \geq M_{R1}\} \right. \\
 & \quad \left. + \Pr\{\mathbb{O}, B_2(i) < M_{R2}, B_1(i) < M_{R1}\} \right] \\
 &= (p_1 + p_2 + p_3) (\mathfrak{o} (f * PU2 + 1 - PU2) \\
 & \quad \times (\mathfrak{g} * PU1 + 1 - PU1)). \quad (72)
 \end{aligned}$$

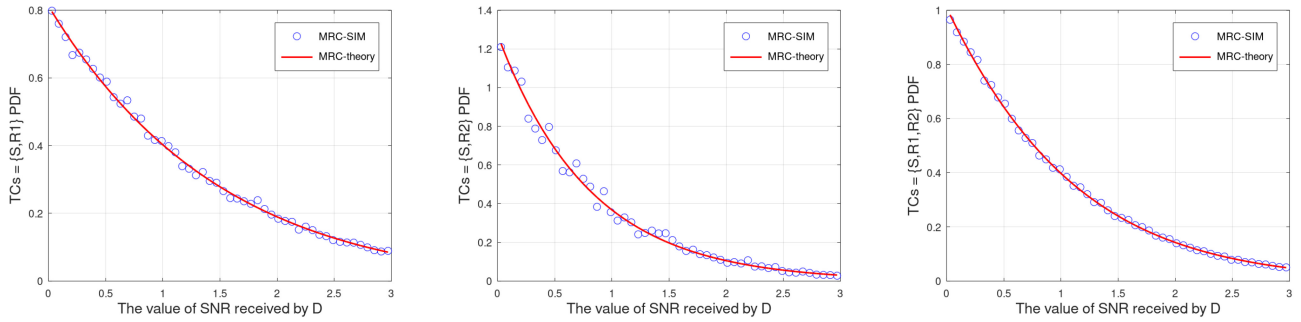


FIGURE 3. PDF of the value of SNR received by D in different TCs with parameters  $1/\lambda_1 = -12$  dB,  $1/\lambda_2 = -15$  dB,  $R_0 = 2$  bit/s/Hz,  $M_1 = 10$  mJoules,  $M_2 = 8$  mJoules.

With the Eq. (59), we get

$$\begin{aligned} \Pr\{B_2(i) < M_{R2}\} &= \int_{x=0}^{M_{R2}} \frac{(1 - e^{-Q_2 x})}{M_{R2}} dx \\ &= 1 - \frac{(e^{Q_2 M_{R2}} - 1)}{Q_2 M_{R2}}. \end{aligned} \quad (73)$$

Due to  $b_2 \lambda_2 e^{Q_2 M_{R2}} = b_2 \lambda_2 + Q_2$ , we get  $e^{Q_2 M_{R2}} = 1 + \frac{Q_2}{b_2 \lambda_2}$ , and thus

$$\begin{aligned} \Pr\{B_2(i) < M_{R2}\} &= 1 - \frac{\left(1 + \frac{Q_2}{b_2 \lambda_2} - 1\right)}{Q_2 M_{R2}} \\ &= 1 - \frac{1}{b_2 \lambda_2 M_{R2}}. \end{aligned} \quad (74)$$

Accordingly, we get

$$\begin{aligned} \Pr\{B_2(i) \geq M_{R2}\} &= 1 - \Pr\{B_2(i) < M_{R2}\} \\ &= \frac{1}{b_2 \lambda_2 M_{R2}} = PU2. \end{aligned} \quad (75)$$

Similarly, with the Eq. (59) and  $b_1 \lambda_1 e^{Q_1 M_{R1}} = b_1 \lambda_1 + Q_1$ , we can get

$$\Pr\{B_1(i) < M_{R1}\} = 1 - \frac{1}{b_1 \lambda_1 M_{R1}}, \quad (76)$$

and

$$\Pr\{B_1(i) \geq M_{R1}\} = \frac{1}{b_1 \lambda_1 M_{R1}} = PU1. \quad (77)$$

With the help of Eq. (47) to Eq. (53) and Eq. (65) as well as Eq. (58) and Eq. (68) to Eq. (72) can be rewritten as follows

$$\begin{aligned} OP &= p_S \left(1 - e^{-W_{SD} \Gamma_{th}}\right) \\ &+ p_{SR1} \left(\mathbf{c} * (\mathbf{d} * PU1 + 1 - PU1)\right) \\ &+ p_{SR2} \left(\mathbf{c} * (\mathbf{n} * PU2 + 1 - PU2)\right) \\ &+ (p_1 + p_2 + p_3) \left(\mathbf{o} (f * PU2 + 1 - PU2)\right. \\ &\quad \left. \times (\mathbf{g} * PU1 + 1 - PU1)\right). \end{aligned} \quad (78)$$

Correspondingly, the throughput of the system  $\tau$  can be defined as

$$\begin{aligned} \tau &= (1 - OP)R_0 \\ &= R_0 \left[1 - \left(p_S \left(1 - e^{-W_{SD} \Gamma_{th}}\right)\right.\right. \\ &\quad \left. + p_{SR1} \left(\mathbf{c} * (\mathbf{d} * PU1 + 1 - PU1)\right)\right. \\ &\quad \left. + p_{SR2} \left(\mathbf{c} * (\mathbf{n} * PU2 + 1 - PU2)\right)\right. \\ &\quad \left. + (p_1 + p_2 + p_3) \left(\mathbf{o} (f * PU2 + 1 - PU2)\right.\right. \\ &\quad \left. \left. \times (\mathbf{g} * PU1 + 1 - PU1)\right)\right]. \end{aligned} \quad (79)$$

Furthermore, the time slot cost for each data  $T_c$  is a performance index worthy of attention. And it can be calculated as follows:

$$\begin{aligned} T_c &= \lim_{N \rightarrow \infty} \sum_{i=1}^N OP^{i-1} (1 - OP) i \\ &= \lim_{N \rightarrow \infty} (1 - OP) \frac{1}{1 - OP} \left[1 + \frac{(OP)(1 - (OP)^{N-1})}{1 - OP} - N(OP)^N\right] \\ &= \frac{1}{1 - OP}. \end{aligned} \quad (80)$$

## V. PERFORMANCE RESULTS

In this section, simulations are presented to verify the rationality of the derived theoretical expressions. In addition, the performance comparisons between our work and existing papers are performed. For all simulations, the following system parameters are taken into account unless otherwise specified. Suppose S, R1, R2, and D are all located on a two-dimensional plane, and their position coordinates are (0,0), (30,20), (60,-20), and (100,0), respectively. Path-loss exponent  $\alpha = -3$ . The transmitting power of S node  $P_{Ts} = 12$  dBm. The channel noise variance  $N_0 = -50$  dBm. With the measure of Alg. 1, the corresponding transmitter candidate set probabilities,  $p_{\gamma_{overall1}}$ ,  $p_{\gamma_{overall2}}$ ,  $p_{\gamma_{overall3}}$ , 'c', 'd', 'f', 'g', 'm', 'n' and 'o' are obtained. Furthermore, in all figures, point markers represent simulation values, and solid red lines indicate the STM-based theoretical values.

In Fig. 3, three subfigures depict the PDF of the value of SNR received by D in different TCs, namely,  $p_{\gamma_{overall1}}$ ,  $p_{\gamma_{overall2}}$ ,  $p_{\gamma_{overall3}}$ . The red solid line represents the theoretic value calculated with Alg. 1. It can be observed that the

**Algorithm 1** Probability  $p_s$ ,  $PSR1$ ,  $PSR2$ ,  $P1$ ,  $P2$ ,  $P3$ ,  $P_{\gamma_{overall1}}$ ,  $P_{\gamma_{overall2}}$ ,  $P_{\gamma_{overall3}}$ , ‘c’, ‘d’, ‘f’, ‘g’, ‘m’, ‘n’ and ‘o’ Based on STM

**Require:**  $W_{SD}, W_{SR1}, W_{SR2}, W_{R1D}, W_{R1R2}, W_{R2D}, \Gamma_{th}, \lambda_1, \lambda_2, M_{R1}, M_{R2}, \mathcal{N}$ .

1: Initialize  $i_4 = 0, k_4 = 0, j_1$  and  $j_2 \in \{1, 2, 3, 4, 5, 6\}$ ,  $p(0) = [p_s, PSR1, PSR2, P1, P2, P3] = [\frac{1}{6}, \frac{1}{6}, \frac{1}{6}, \frac{1}{6}, \frac{1}{6}, \frac{1}{6}]$ ,  $PU1 = PU2 = \frac{1}{2}$ .

2: **while** 1 **do**

3: Calculate  $T1(i_4)$  and  $T2(i_4)$  according to equations from Eq. (36) to Eq. (39),

4:  $i_1 = 0, k_1 = 0$

5:  $P_{\gamma_{overall1}}(0) = [P_{\gamma_{overall1}}(1), \dots, P_{\gamma_{overall1}}(\mathcal{N})]$

6:  $P_{\gamma_{overall1}}(j) = \frac{1}{\mathcal{N}}, 1 \leq j \leq \mathcal{N}$  and  $j \in Z$

7: **while** 1 **do**

8:  $P_{\gamma_{overall1}}(i_1 + 1) = P_{\gamma_{overall1}}(i_1)T1(i_4)$ ,

9: **if** ( $P_{\gamma_{overall1}}(i) \leq 0 \mid T1(i_4) < 0$ ) **then**

10:  $k_1 = i_1 - 1$ ,

11: **break**,

12: **else if** ( $\|P_{\gamma_{overall1}}(i_1) - P_{\gamma_{overall1}}(i_1 + 1)\|_2 < 10^{-7}$ ) **then**

13:  $k_1 = i_1$ ,

14: **break**,

15: **else**

16:  $i_1 = i_1 + 1$ ,

17: **end if**

18: **end while**

19:  $P_{\gamma_{overall1}} = P_{\gamma_{overall1}}(k_1)$

20:

21:  $i_2 = 0, k_2 = 0$

22:  $P_{\gamma_{overall2}}(0) = [P_{\gamma_{overall2}}(1), \dots, P_{\gamma_{overall2}}(\mathcal{N})]$

23:  $P_{\gamma_{overall2}}(j) = \frac{1}{\mathcal{N}}, 1 \leq j \leq \mathcal{N}$  and  $j \in Z$

24: **while** 1 **do**

25:  $P_{\gamma_{overall2}}(i_2 + 1) = P_{\gamma_{overall2}}(i_2)T2(i_4)$ ,

26: **if** ( $P_{\gamma_{overall2}}(i) \leq 0 \mid T2(i_4) < 0$ ) **then**

27:  $k_2 = i_2 - 1$ ,

28: **break**,

29: **else if** ( $\|P_{\gamma_{overall2}}(i_2) - P_{\gamma_{overall2}}(i_2 + 1)\|_2 < 10^{-7}$ ) **then**

30:  $k_2 = i_2$ ,

31: **break**,

32: **else**

33:  $i_2 = i_2 + 1$ ,

34: **end if**

35: **end while**

36:  $P_{\gamma_{overall2}} = P_{\gamma_{overall2}}(k_2)$

37:

38: Calculate  $T3(i_4)$ ,  $P_{d_{S \rightarrow R2}}$  and  $P_{d_{R1 \rightarrow R2}}$  according to equations from Eq. (40) to Eq. (45),

39:  $i_3 = 0, k_3 = 0$

40:  $P_{\gamma_{overall3}}(0) = [P_{\gamma_{overall3}}(1), \dots, P_{\gamma_{overall3}}(\mathcal{N})]$

41:  $P_{\gamma_{overall3}}(j) = \frac{1}{\mathcal{N}}, 1 \leq j \leq \mathcal{N}$  and  $j \in Z$

42: **while** 1 **do**

43:  $P_{\gamma_{overall3}}(i_3 + 1) = P_{\gamma_{overall3}}(i_3)T3(i_4)$ ,

44: **if** ( $P_{\gamma_{overall3}}(i) \leq 0 \mid T3(i_4) < 0$ ) **then**

45:  $k_3 = i_3 - 1$ ,

46: **break**,

47: **else if** ( $\|P_{\gamma_{overall3}}(i_3) - P_{\gamma_{overall3}}(i_3 + 1)\|_2 < 10^{-7}$ ) **then**

48:  $k_3 = i_3$ ,

49: **break**,

50: **else**

51:  $i_3 = i_3 + 1$ ,

52: **end if**

53: **end while**

54:  $P_{\gamma_{overall3}} = P_{\gamma_{overall3}}(k_3)$

55: Calculate ‘c’, ‘d’, ‘f’, ‘g’, ‘m’, ‘n’ and ‘o’ and equations from Eq. (46) to Eq. (53),

56: Calculate  $T(i)$  according to  $p(i)$  and equations from Eq. (20) to Eq. (35),

57:  $p(i_4 + 1) = p(i_4)T(i_4)$ ,

58: **if** ( $p_{j_1}(i) \leq 0 \mid T_{j_1 j_2}(i_4) < 0$ ) **then**

59:  $k_4 = i_4 - 1$ ,

60: **break**,

61: **else if** ( $\|p(i_4) - p(i_4 + 1)\|_2 < 10^{-7}$ ) **then**

62:  $k_4 = i_4$ ,

63: **break**,

64: **else**

65:  $i_4 = i_4 + 1$ ,

66: **end if**

67: **end while**

**Ensure:** Probability Distribution  $p(k_4)$ ,  $P_{\gamma_{overall1}}$ ,  $P_{\gamma_{overall2}}$ ,  $P_{\gamma_{overall3}}$ , ‘c’, ‘d’, ‘f’, ‘g’, ‘m’, ‘n’ and ‘o’.

simulation values, represented by the blue circle markers, lay on the red solid line, which shows the rationality of the Alg. 1.

Fig. 4 and Fig. 5 depict the limiting PDF of energy stored in the R1 buffer and R2 buffer, obtained by simulation and theoretical analysis. It can be clearly seen from Fig. 4 that

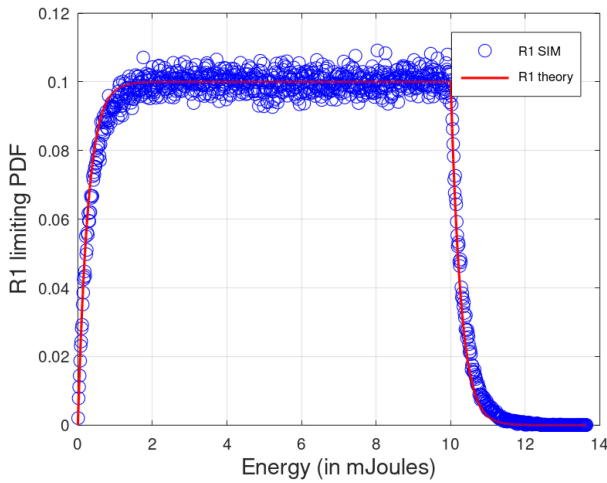


**FIGURE 4.** Limiting distribution of energy with infinite-size PEB of relay 1 and parameters  $1/\lambda_1 = -15$  dB,  $1/\lambda_2 = -12$  dB,  $R_0 = 2$  bit/s/Hz,  $M_1 = 10$  mJoules,  $M_2 = 8$  mJoules.

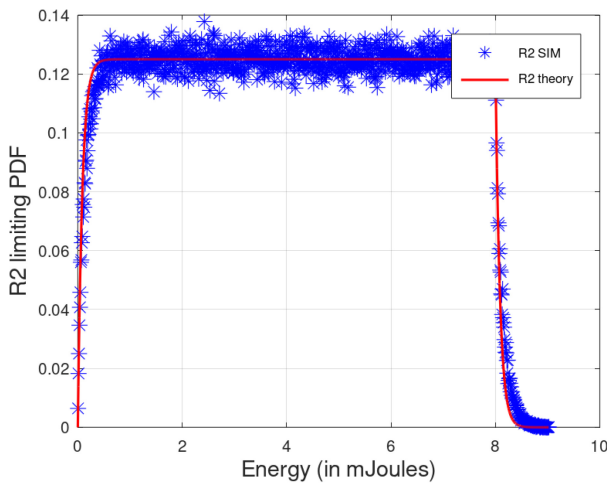


**FIGURE 5.** Limiting distribution of energy with finite-size PEB of relay 2 and parameters  $1/\lambda_1 = -15$  dB,  $1/\lambda_2 = -12$  dB,  $R_0 = 2$  bit/s/Hz,  $M_1 = 10$  mJoules,  $M_2 = 8$  mJoules.

the solid line and dashed line almost exactly coincide, and they are almost in the middle of the simulation values. Furthermore, the same case can be seen in Fig. 5, which effectively proves the accuracy of the derived theoretical expressions in Eq. (66) and Eq. (57).

In Fig. 6, six cooperative communication networks are shown, which are MRC system proposed in our paper, Non-MRC system proposed in [19], IBEP and IOFP proposed in [10], SBRB proposed in [11] and BSCSI proposed in [25]. It can be observed that IBEP, IOFP, SBRB, and BSCSI systems are outage regardless of the value of  $P_S$ , when all parameters are the same as the MRC system. Fig. 6 shows the system outage probability of the system applied MRC obviously less than Non-MRC system. And the outage probability of our system is the least among these networks. In addition, Fig. 7 depicts the throughput of system and our system also outperform to Non-MRC system. This is

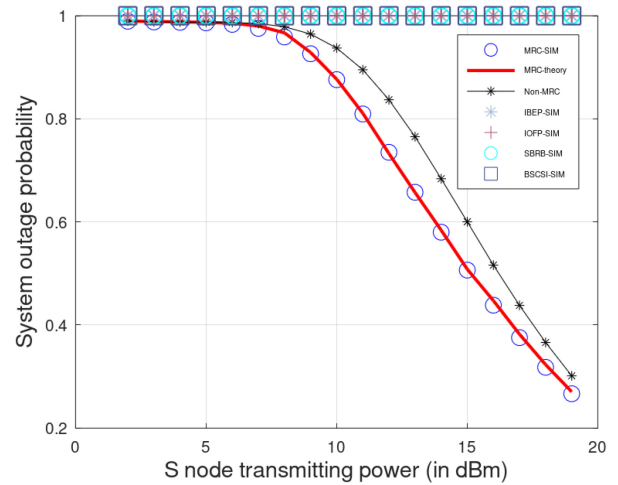


**FIGURE 6.** Outage probability of system vs.  $P_{T_S}$ , with parameters  $1/\lambda_1 = -11$  dB,  $1/\lambda_2 = -12$  dB,  $R_0 = 2$  bit/s/Hz,  $M_1 = 12$  mJoules,  $M_2 = 10$  mJoules.

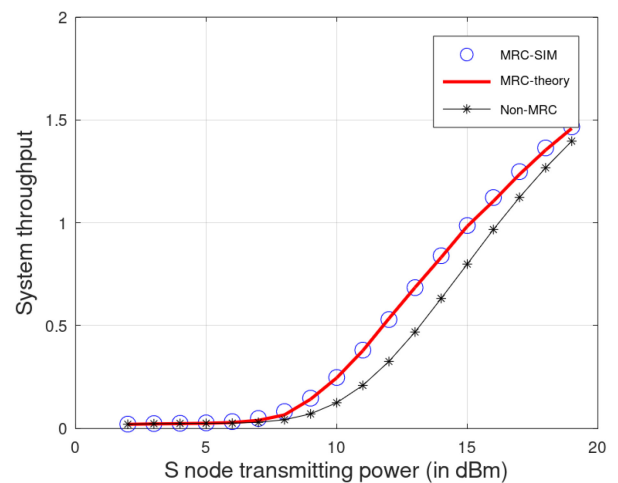


**FIGURE 7.** Throughput of system vs.  $P_{T_S}$ , with parameters  $1/\lambda_1 = -11$  dB,  $1/\lambda_2 = -12$  dB,  $R_0 = 2$  bit/s/Hz,  $M_1 = 12$  mJoules,  $M_2 = 10$  mJoules.

because the MRC algorithm can combine the multipath signal with the appropriate coefficient to achieve diversity gain. Furthermore, it can be observed that the outage and throughput change slightly, when  $P_{T_S}$  is from 2 dBm to 8 dBm, and change considerably when  $P_{T_S}$  is from 9 dBm to 19 dBm. The reason for this phenomenon is that, when  $P_{T_S}$  is small, it is difficult for S node transmitting data packet reliably to any other node, in other words, in the whole system, only S node is activated in most time. With the increase in  $P_{T_S}$ , S node is able to transmit the data packet to relay nodes. With the help of relay nodes, the performance of system improves substantially.

In Fig. 8, the system time slot cost for each data are demonstrated. These simulations can clarify that the MRC system outperforms the Non-MRC system. Furthermore, it can be seen that time slot cost of MRC system is close to that of Non-MRC system when  $P_{T_S}$  is from 2 dBm to 4 dBm and from 14 dBm to 19dBm. This is because, when  $P_{T_S}$  is too

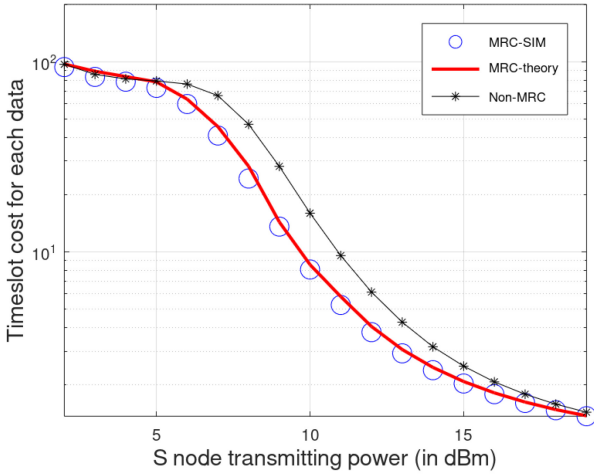


**FIGURE 8.** Time slot cost for each data vs.  $P_{TS}$ , with parameters  $1/\lambda_1 = -11$  dB,  $1/\lambda_2 = -12$  dB,  $R_0 = 2$  bit/s/Hz,  $M_1 = 12$  mJoules,  $M_2 = 10$  mJoules.

small, the SNR of the signals combined is also too small to reach the SNR threshold and transmit the data packet. As a result, the effect of MRC is not obvious. And when  $P_{TS}$  is too large, even the Non-MRC system can transmit the data packet to D easily so that the effect of MRC is not significant. Thus, if  $P_{TS}$  is from 5 dBm to 13 dBm, the Non-MRC system is hard to utilize the SNR of single signal to reach SNR threshold, however, our MRC system can exploit the SNR of multiple signals combined to finish the data packet transmitting. Hence, in these cases, MRC significantly improves system performance.

## VI. CONCLUSION

This paper combines OR aided cooperative communication network with EH nodes and MRC. By applying the discrete-time continuous-state space Markov chain model, the theoretical algorithm-based expressions for limiting the distributions of stored energy in infinite-size buffers are derived. Furthermore, by using both the limiting distributions of energy buffers and data-broadcasted probability at nodes, the theoretical numerical expressions for outage probability and throughput of the network are obtained. In the future, combining the generalized selection combining (GSC) with OR under the assumption of an EH cooperative communication network is worth being studied.

## APPENDIX A

### ALGORITHM FOR PROBABILITY $P_S, P_{SR1}, P_{SR2}, P_1, P_2, P_3, P_{YOVERALL1}, P_{YOVERALL2}, P_{YOVERALL3}, \mathcal{C}, \mathcal{D}, \mathcal{F}, \mathcal{G}, \mathcal{M}, \mathcal{N}, \mathcal{O}$ AND $\mathcal{Q}$ BASED ON STM

Specifically, in line 9, 26, 44 and 58, the judgment condition ( $p(i) \leq 0 | T(i) < 0$ ) indicates that there are non-positive elements in  $p(i)$  or  $T(i)$ , which is not desirable, so the update process needs to be terminated. Moreover, in line 12, 29, 47 and 61, ( $\|p(i) - p(i+1)\|_2 < 10^{-7}$ ) indicates that the update error is small enough and the update process has converged. Therefore, the update process can be terminated.

## APPENDIX B PROOF OF THEOREM 1

According to the total probability theorem,  $\mathbb{P}_{21}$  and  $\mathbb{P}_{22}$ , the CDF of  $B_2(i+1)$  in storage process in Eq. (54) may be evaluated as follows

$$\begin{aligned}
 & \Pr\{B_2(i+1) \leq x\} \\
 &= \Pr\{B_2(i) + X(i) \leq x, TCs = \{S\}\} \\
 &+ \Pr\{B_2(i) + X(i) \leq x, TCs = \{S, R1\}\} \\
 &+ \Pr\{B_2(i) + X(i) \leq x, TCs = \{S, R2\}, B_2(i) < M_{R2}\} \\
 &+ \Pr\{B_2(i) + X(i) \leq x, TCs = \{S, R2\}, B_2(i) \geq M_{R2}, \mathbb{M}, \mathbb{N}\} \\
 &+ \Pr\{B_2(i) + X(i) \leq x, TCs = \{S, R2\}, B_2(i) \geq M_{R2}, \overline{\mathbb{C}}\} \\
 &+ \Pr\{B_2(i) + X(i) \leq x, TCs = \{S, R1, R2\}, \\
 &\quad B_2(i) \geq M_{R2}, \mathbb{O}, \mathbb{F}\} \\
 &+ \Pr\{B_2(i) + X(i) \leq x, TCs = \{S, R1, R2\}, \\
 &\quad B_2(i) \geq M_{R2}, \overline{\mathbb{O}}\} \\
 &+ \Pr\{B_2(i) + X(i) \leq x, TCs = \{S, R1, R2\}, B_2(i) < M_{R2}\} \\
 &+ \Pr\{B_2(i) - M_{R2} + X(i) \leq x, TCs = \{S, R2\}, \\
 &\quad B_2(i) \geq M_{R2}, \mathbb{M}, \overline{\mathbb{N}}\} \\
 &+ \Pr\{B_2(i) - M_{R2} + X(i) \leq x, TCs = \{S, R1, R2\}, \\
 &\quad B_2(i) \geq M_{R2}, \mathbb{O}, \overline{\mathbb{F}}\}, \tag{81}
 \end{aligned}$$

When  $i \rightarrow \infty$ , the equation  $\Pr\{B_2(i+1) \leq x\} = G_2^{i+1}(x) = G_2^i(x) = G_2(x)$  holds for the steady state of energy buffer at RNs. Thus, Eq. (81) can be written as follows

$$\begin{aligned}
 G_2(x) &= (p_S + p_{SR1}) \int_{\mu_2=0}^x F_X(x - \mu_2) g_2(\mu_2) d\mu_2 \\
 &+ (p_{SR2} * (\mathbf{m} * \mathbf{n} + 1 - \mathbf{m}) \\
 &\quad + (p_1 + p_2 + p_3)(\mathbf{o} * \mathbf{f} + 1 - \mathbf{o})) \\
 &\times \int_{\mu_2=M_{R2}}^x F_X(x - \mu_2) g_2(\mu_2) d\mu_2 \\
 &+ (p_{SR2} + p_{SR1R2}) \int_{\mu_2=0}^{\min(x, M_{R2})} F_X(x - \mu_2) g_2(\mu_2) d\mu_2 \\
 &+ (p_{SR2} * \mathbf{m} * (1 - \mathbf{n}) + (p_1 + p_2 + p_3) * \mathbf{o} * (1 - \mathbf{f})) \\
 &\times \int_{\mu_2=M_{R2}}^{x+M_{R2}} F_X(x + M_{R2} - \mu_2) g_2(\mu_2) d\mu_2, \tag{82}
 \end{aligned}$$

where  $g_2(x)$  is the derivative of  $G_2(x)$ . With simplifying Eq. (82), we arrive at

$$G_2(x) = \begin{cases} G_{21}(x), & 0 \leq x < M_{R2} \\ G_{22}(x), & x \geq M_{R2} \end{cases} \tag{83}$$

where,

$$\begin{aligned}
 G_{21}(x) &= b_2 \int_{\mu_2=M_{R2}}^{x+M_{R2}} F_X(x + M_{R2} - \mu_2) g_1(\mu_2) d\mu_2 \\
 &+ \int_{\mu_2=0}^x F_X(x - \mu_2) g_1(\mu_2) d\mu_2, 0 \leq x < M_{R2} \tag{84}
 \end{aligned}$$

$$G_{22}(x) = \int_{\mu_2=0}^{M_{R2}} F_X(x - \mu_2)g_2(\mu_2) d\mu_2 + a_2 \int_{\mu_2=M_{R2}}^x F_X(x - \mu_2)g_2(\mu_2) d\mu_2 + b_2 \int_{\mu_2=M_{R2}}^{x+M_{R2}} F_X(x + M_{R2} - \mu_2)g_2(\mu_2) d\mu_2, \quad x \geq M_{R2} \quad (85)$$

where,

$$a_2 = p_S + p_{SR1} + p_{SR2} * m * n + (p_1 + p_2 + p_3)(o * f + (1 - o)) + p_{SR2} * (1 - m), \quad (86)$$

$$b_2 = p_{SR2} * m(1 - n) + (p_1 + p_2 + p_3) * o(1 - f). \quad (87)$$

According to Eq. (83), the PDF  $g_2(x)$  may be defined as

$$g_2(x) = \begin{cases} g_{21}(x), & 0 \leq x < M_{R2} \\ g_{22}(x), & x \geq M_{R2}. \end{cases} \quad (88)$$

Substituting Eq. (88) into Eq. (85), the derivatives about  $x$  on both sides of Eq. (85) can be obtained as follows

$$g_{22}(x) = \int_{\mu_1=0}^{M_{R2}} f_X(x - \mu_2)g_{21}(\mu_2) d\mu_2 + a_2 \int_{\mu_1=M_{R2}}^x f_X(x - \mu_2)g_{22}(\mu_2) d\mu_2 + b_2 \times \int_{\mu_1=M_{R2}}^{x+M_{R2}} f_X(x + M_{R2} - \mu_2)g_{22}(\mu_2) d\mu_2, \quad x \geq M_{R2} \quad (89)$$

Obviously,  $a_2 + b_2 = 1$ . In addition, with [6], it is declared that, when  $M_{R2} > \mathbb{E}[X(i)] = 1/\lambda_2$ , the energy update process in Eq. (54) possesses a unique stationary distribution, namely,  $g_2(x)$  has unique solution. Furthermore, from [6],  $g_{22}(x)$  can be assumed to have an exponential form solution, which can be expressed by  $g_{22}(x) = k_2 e^{Q_2 x}$ . Substituting  $g_{22}(x) = k_2 e^{Q_2 x}$  and  $f_X(x) = \lambda_2 e^{-\lambda_2 x}$  into Eq. (89), we obtain

$$k_2 e^{Q_2 x} = \int_{\mu_2=0}^{M_{R2}} \lambda_2 e^{-\lambda_2(x-\mu_2)} g_{21}(\mu_2) d\mu_2 + a_2 \int_{\mu_1=M_{R2}}^x \lambda_2 e^{-\lambda_2(x-\mu_2)} k_2 e^{Q_2 \mu_2} d\mu_2 + b_2 \times \int_{\mu_1=M_{R2}}^{x+M_{R2}} \lambda_2 e^{-\lambda_2(x+M_{R2}-\mu_2)} k_2 e^{Q_2 \mu_2} d\mu_2, \quad x \geq M_{R2} \quad (90)$$

Simplifying Eq. (90), we obtain

$$k_2 e^{Q_2 x} = \lambda_2 e^{-\lambda_2 x} \int_{\mu_2=0}^{M_{R2}} e^{\lambda_2 \mu_2} g_{21}(\mu_2) d\mu_2 - \frac{k_2 \lambda_2 e^{(Q_2 M_{R2} - \lambda_2 x)} (a_2 e^{\lambda_2 M_{R2}} + b_2)}{\lambda_2 + Q_2} + \frac{\lambda_2 (a_2 + b_2 e^{Q_2 M_{R2}}) k_2 e^{Q_2 x}}{\lambda_2 + Q_2}, \quad x \geq M_{R2} \quad (91)$$

For Eq. (91) to hold, the following conditions need to be satisfied

$$\begin{cases} \frac{\lambda_2 (a_2 + b_2 e^{Q_2 M_{R2}})}{\lambda_2 + Q_2} = 1, & (92a) \\ \frac{k_2 e^{Q_2 M_{R2}} (a_2 e^{\lambda_2 M_{R2}} + b_2)}{\lambda_2 + Q_2} = \int_{\mu_2=0}^{M_{R2}} e^{\lambda_2 \mu_2} g_{21}(\mu_2) d\mu_2. & (92b) \end{cases}$$

The desirable solution  $Q_2$  of Eq. (92a) for the finite distribution of  $g_{22}(x)$  may be obtained by simplifying Eq. (92a) as follows

$$b_2 \lambda_2 e^{Q_2 M_{R2}} = \lambda_2 - a_2 \lambda_2 + Q_2 = b_2 \lambda_2 + Q_2, \quad (93)$$

Although, it can be easily found from Eq. (92a) that  $Q_{20} = 0$  is one of the solutions of  $Q_2$  in Eq. (92a),  $Q_{20}$  does not satisfy the condition that  $g_{22}(x)$  is a limiting distribution. And the other solution  $Q_{21}$  of  $Q_2$  in Eq. (92a) can be obtained by simplifying Eq. (92a) as

$$Q_2 = \frac{-W(-b_2 \lambda_2 M_{R2} e^{-b_2 \lambda_2 M_{R2}})}{M_{R2}} - b_2 \lambda_2, \quad b_2 \lambda_2 M_{R2} > 1. \quad (94)$$

where, with  $b_2 \lambda_2 M_{R2} > 1$ ,  $W(-b_2 \lambda_2 M_{R2} e^{-b_2 \lambda_2 M_{R2}}) > -b_2 \lambda_2 M_{R2}$  so that  $Q_2 < 0$ , ensuring the finite distribution of  $g_{22}(x)$ .

Correspondingly, when  $0 \leq x < M_{R2}$ , substitute Eq. (88) into Eq. (84) and differentiate both sides of Eq. (84) with respect to  $x$ . we have

$$g_{21}(x) = b_2 \int_{\mu_2=M_{R2}}^{x+M_{R2}} f_X(x + M_{R2} - \mu_2)g_{22}(\mu_2) d\mu_2 + \int_{\mu_2=0}^x f_X(x - \mu_2)g_{21}(\mu_2) d\mu_2, \quad 0 \leq x < M_{R2} \quad (95)$$

Substituting  $g_{22}(x) = k_2 e^{Q_2 x}$  and  $f_X(x) = \lambda_2 e^{-\lambda_2 x}$  into Eq. (95), we get

$$g_{21}(x) = \lambda_2 \int_{\mu_2=0}^x e^{-\lambda_2(x-\mu_2)} g_{21}(\mu_2) d\mu_2 + \frac{b_2 k_2 \lambda_2 e^{Q_2 M_{R2}}}{\lambda_2 + Q_2} (e^{Q_2 x} - e^{-\lambda_2 x}), \quad 0 \leq x < M_{R2} \quad (96)$$

Let  $r(x) = \frac{b_2 k_2 \lambda_2 e^{Q_2 M_{R2}}}{\lambda_2 + Q_2} (e^{Q_2 x} - e^{-\lambda_2 x})$ , and the integral equation in Eq. (96) can be rewritten as follows

$$g_{21}(x) = \lambda_2 \int_{\mu_2=0}^x e^{-\lambda_2(x-\mu_2)} g_{21}(\mu_2) d\mu_2 + r(x), \quad 0 \leq x < M_{R2} \quad (97)$$

Clearly, Eq. (97) is a Volterra integral equation of the second kind, whose solution is given by [6], [7] and [23, eq. 2.2.1]

$$g_{21}(x) = r(x) + \lambda_2 \int_{t=0}^x r(t) dt, \quad (98)$$

Substituting  $r(x)$  into Eq. (98), we obtain

$$\begin{aligned} g_{21}(x) &= \frac{b_2 k_2 \lambda_2 e^{Q_2 M_{R2}}}{\lambda_2 + Q_2} (e^{Q_2 x} - e^{-\lambda_2 x}) \\ &\quad + \lambda_2 \int_{t=0}^x \frac{b_2 k_2 \lambda_2 e^{Q_2 M_{R2}}}{\lambda_2 + Q_2} (e^{Q_2 t} - e^{-\lambda_2 t}) dt \\ &= \frac{b_2 k_2 \lambda_2 e^{Q_2 M_{R2}} (e^{Q_2 x} - 1)}{Q_2}, 0 \leq x < M_{R2} \end{aligned} \quad (99)$$

Because of the unit area condition on  $g_2(x)$ , we have

$$\int_{x=0}^{\infty} g_2(x) dx = \int_{x=0}^{M_{R2}} g_{21}(x) dx + \int_{x=M_{R2}}^{\infty} g_{22}(x) dx = 1, \quad (100)$$

Substituting  $g_{21}(x) = \frac{b_2 k_2 \lambda_2 e^{Q_2 M_{R2}} (e^{Q_2 x} - 1)}{Q_2}$  and  $g_{22}(x) = k_2 e^{Q_2 x}$  into Eq. (100), we arrive at

$$k_2 = \frac{-Q_2}{M_{R2}(b_2 \lambda_2 + Q_2)}, \quad (101)$$

Furthermore, according to Eq. (101), we have

$$g_{21}(x) = \frac{1 - e^{Q_2 x}}{M_{R2}}. \quad (102)$$

Substituting Eq. (102) into the right side of Eq. (92b), we obtain

$$\begin{aligned} \int_{\mu_2=0}^{M_{R2}} e^{\lambda_2 \mu_2} g_{21}(\mu_2) d\mu_2 &= \int_{\mu_2=0}^{M_{R2}} \frac{(1 - e^{Q_2 x}) e^{\lambda_2 \mu_2}}{M_{R2}} d\mu_2 \\ &= \frac{1 - e^{(\lambda_2 + Q_2) M_{R2}}}{(\lambda_2 + Q_2) M_{R2}} - \frac{1 - e^{\lambda_2 M_{R2}}}{\lambda_2 M_{R2}}, \end{aligned} \quad (103)$$

The equation in Eq. (92a) leads us to conclude  $\lambda_2 M_{R2} = \frac{(\lambda_2 + Q_2) M_{R2}}{b_2 e^{Q_2 M_{R2}} + a_2}$ . Substituting this conclusion in Eq. (103), we have

$$\int_{\mu_2=0}^{M_{R2}} e^{\lambda_2 \mu_2} g_{21}(\mu_2) d\mu_2 = \frac{(1 - e^{Q_2 M_{R2}})(b_2 + a_2 e^{\lambda_2 M_{R2}})}{(\lambda_2 + Q_2) M_{R2}}, \quad (104)$$

Similarly, the conclude  $1 - e^{Q_2 M_{R2}} = \frac{-Q_2}{b_2 \lambda_2}$  may be obtained from Eq. (93). Substituting this conclusion in Eq. (104), we arrive at

$$\begin{aligned} \int_{\mu_2=0}^{M_{R2}} e^{\lambda_2 \mu_2} g_{21}(\mu_2) d\mu_2 &= \frac{(1 - e^{Q_2 M_{R2}})(b_2 + a_2 e^{\lambda_2 M_{R2}})}{(\lambda_2 + Q_2) M_{R2}} \\ &= \frac{-Q_2 (b_2 + a_2 e^{\lambda_2 M_{R2}})}{(\lambda_2 + Q_2) M_{R2} b_2 \lambda_2} \\ &= \frac{-Q_2 e^{Q_2 M_{R2}} (b_2 + a_2 e^{\lambda_2 M_{R2}})}{M_{R2} (b_2 \lambda_2 + Q_2) (\lambda_2 + Q_2)} \\ &= \frac{k_2 e^{Q_2 M_{R2}} (b_2 + a_2 e^{\lambda_2 M_{R2}})}{\lambda_2 + Q_2}. \end{aligned} \quad (105)$$

Now, the validation of Eq. (92b) in Eq. (105) indicates that the unique solution  $g_{21}(x)$  in Eq. (102) for Eq. (95) and the unique solution  $g_{22}(x) = k_2 e^{Q_2 x}$  for Eq. (89) are obtained.

## APPENDIX C PROOF OF THEOREM 2

According to the energy storage process  $B_2(i)$  with the infinite-size energy buffer in Eq. (61), the variable  $O_R(i)$  is defined by

$$O_R(i) = \begin{cases} 1, & \mathbb{P}_{I1} \\ 0, & \mathbb{P}_{II1} \end{cases} \quad (106)$$

where  $\mathbb{P}_{I1}$  and  $\mathbb{P}_{II1}$  are the conditions required for the equations in Eq. (106) to hold. Specifically, they can be expressed as follows

$$\begin{aligned} \mathbb{P}_{I1} &: [(TCs = \{S, R2\}) \cap \mathbb{C} \cap \bar{\mathbb{N}}] \\ &\quad \cup [(TCs = \{S, R1, R2\}) \cap \mathbb{O} \cap \bar{\mathbb{F}}], \\ \mathbb{P}_{II1} &: (TCs = \{S\}) \cup (TCs = \{S, R1\}) \\ &\quad \cup [(TCs = \{S, R2\}) \cap \mathbb{C} \cap \bar{\mathbb{N}}] \\ &\quad \cup [(TCs = \{S, R2\}) \cap \bar{\mathbb{C}}] \\ &\quad \cup [(TCs = \{S, R1, R2\}) \cap \mathbb{O} \cap \bar{\mathbb{F}}] \\ &\quad \cup [(TCs = \{S, R1, R2\}) \cap \bar{\mathbb{O}}]. \end{aligned} \quad (108)$$

Moreover, the variable  $\theta(i)$  is defined as follows

$$\theta(i) = \begin{cases} 1, & B_2(i) \geq M_{R2} \\ 0, & B_2(i) < M_{R2} \end{cases} \quad (109)$$

Implying Eq. (106), Eq. (107), Eq. (108) and Eq. (109), the energy storage process in Eq. (61) can be re-expressed as follows

$$B_2(i+1) - B_2(i) = X(i) - M_{R2} \theta(i) O_R(i). \quad (110)$$

According to the law of large numbers, the average energy harvesting rate can be obtained as follows

$$\mathbb{E}[X(i)] = \lim_{N \rightarrow \infty} \frac{1}{N} \sum_{i=1}^N X(i), \quad (111)$$

Similarly, the average energy consumption rate can be given by

$$\begin{aligned} \mathbb{E}[M_{R2} \theta(i) O_R(i)] &= \lim_{N \rightarrow \infty} \frac{1}{N} \sum_{i=1}^N M_{R2} \theta(i) O_R(i) \\ &= \lim_{N \rightarrow \infty} \frac{1}{N} \sum_{B_2(i) \geq M_{R2}} M_{R2} O_R(i) \\ &\leq M_{R2} \left\{ \lim_{N \rightarrow \infty} \frac{1}{N} \sum_{i=1}^N O_R(i) \right\}, \end{aligned} \quad (112)$$

And,

$$\begin{aligned} \mathbb{E}[O_R(i)] &= \lim_{N \rightarrow \infty} \frac{1}{N} \sum_{i=1}^N O_R(i) \\ &= 1 \times \Pr\{O_R(i) = 1\} + 0 \times \Pr\{O_R(i) = 0\} \\ &= \Pr\{B_2(i) - M_{R2} + X(i) \leq x, TCs = \{S, R2\}, \\ &\quad B_2(i) \geq M_{R2}, \mathbb{M}, \bar{\mathbb{N}}\} \end{aligned}$$



$$\begin{aligned}
 & + \Pr\left\{B_2(i) - M_{R2} + X(i) \leq x, TCs = \{S, R1, R2\}, \right. \\
 & \quad \left. B_2(i) \geq M_{R2}, \mathbb{O}, \overline{\mathbb{F}}\right\} \\
 & = b_2, \tag{113}
 \end{aligned}$$

From Eq. (112) and Eq. (113), we obtain

$$\mathbb{E}[M_{R2}\theta(i)O_R(i)] \leq b_1. \tag{114}$$

If  $\psi_{R2} \leq 1$ , from Eq. (57), we get

$$\mathbb{E}[X(i)] \geq M_{R2}b_2, \tag{115}$$

Therefore, if  $\psi_1 \leq 1$ , from Eq. (111), Eq. (112), Eq. (114) and Eq. (115), we obtain

$$\lim_{N \rightarrow \infty} \frac{1}{N} \sum_{i=1}^N X(i) \geq \lim_{N \rightarrow \infty} \frac{1}{N} \sum_{i=1}^N M_{R2}\theta(i)O_R(i), \tag{116}$$

According to Eq. (110) and Eq. (116), we have

$$\lim_{N \rightarrow \infty} \frac{1}{N} \sum_{i=1}^N B_2(i+1) \geq \lim_{N \rightarrow \infty} \frac{1}{N} \sum_{i=1}^N B_2(i), \tag{117}$$

Clearly, if the inequality condition holds in Eq. (117), the comparison of between  $B_1(i+1)$  and  $B_1(i)$  shows that the energy accumulates in the buffer over time slot, i.e.,  $\lim_{i \rightarrow \infty} \mathbb{E}[B_1(i)] = \infty$ . Therefore, the stationary distribution of  $B_1(i)$  does not exist, and after a finite number of time slots,  $B_1(i) > M_{R1}$  almost always hold. In addition, if the equality condition holds in Eq. (116), according to Eq. (116) and Eq. (112), we get

$$\lim_{N \rightarrow \infty} \frac{1}{N} \sum_{i=1}^N X(i) = \lim_{N \rightarrow \infty} \frac{1}{N} \sum_{B_2(i) \geq M_{R2}} M_{R2}O_R(i). \tag{118}$$

Eq. (118) indicates that in the energy buffer with DCSMC model, the average energy harvesting rate equals the average energy consumption rate, which is unstable [24]. Therefore, the buffer may almost always provide  $M_{R2}$  amount of energy.

## APPENDIX D PROOF OF THEOREM 3

On the basis of the total probability theorem,  $\mathbb{P}_{11}$  and  $\mathbb{P}_{12}$  form a complete set of events accompanying event  $B_1(i+1)$ . Thus, the cumulative distribution function (CDF) of  $B_1(i+1)$  in the energy update process in Eq. (61) can be expressed as follows

$$\begin{aligned}
 & \Pr\{B_1(i+1) \leq x\} \\
 & = \Pr\{B_1(i) + X(i) \leq x, TCs = \{S\}\} \\
 & + \Pr\{B_1(i) + X(i) \leq x, TCs = \{S, R2\}\} \\
 & + \Pr\{B_1(i) + X(i) \leq x, (TCs = \{S, R1\}), (B_1(i) < M_{R1})\} \\
 & + \Pr\{B_1(i) + X(i) \leq x, (TCs = \{S, R1\}), (B_1(i) \geq M_{R1}, \\
 & \quad \mathbb{C}, \mathbb{D}, \gamma_{SR2}(i) \geq \Gamma_{th}, )\} \\
 & + \Pr\{B_1(i) + X(i) \leq x, (TCs = \{S, R1\}), (B_1(i) \geq M_{R1}, \\
 & \quad \mathbb{C}, \mathbb{D}, \gamma_{SR2}(i) < \Gamma_{th}, \gamma_{R1R2}(i) < \Gamma_{th})\}
 \end{aligned}$$

$$\begin{aligned}
 & + \Pr\left\{B_1(i) + X(i) \leq x, (TCs = \{S, R1, R2\}), \right. \\
 & \quad \left. (B_2(i) \geq M_{R2}, \mathbb{O}, \overline{\mathbb{F}})\right\} \\
 & + \Pr\{B_1(i) + X(i) \leq x, (TCs = \{S, R1, R2\}), \\
 & \quad (B_2(i) \geq M_{R2}, \mathbb{O}, \overline{\mathbb{F}}, B_1(i) \geq M_{R1}, \mathbb{G})\} \\
 & + \Pr\{B_1(i) + X(i) \leq x, (TCs = \{S, R1, R2\}), \\
 & \quad (B_2(i) \geq M_{R2}, \mathbb{O}, \overline{\mathbb{F}}, B_1(i) < M_{R1})\} \\
 & + \Pr\left\{B_1(i) - M_{R1} + X(i) \leq x, \right. \\
 & \quad \left. (TCs = \{S, R1\}), (B_1(i) \geq M_{R1}), \mathbb{C}, \overline{\mathbb{D}}\right\} \\
 & + \Pr\{B_1(i) - M_{R1} + X(i) \leq x, \\
 & \quad (TCs = \{S, R1\}), ((B_1(i) \geq M_{R1}), \mathbb{C}, \mathbb{D}, \\
 & \quad \gamma_{SR2}(i) < \Gamma_{th}, \gamma_{R1R2}(i) \geq \Gamma_{th})\} \\
 & + \Pr\left\{B_1(i) - M_{R1} + X(i) \leq x, (TCs = \{S, R1, R2\}), \right. \\
 & \quad \left. (B_2(i) \geq M_{R2}, \mathbb{O}, \overline{\mathbb{F}}, (B_1(i) \geq M_{R1}), \overline{\mathbb{G}})\right\} \\
 & + \Pr\left\{B_1(i) - M_{R1} + X(i) \leq x, (TCs = \{S, R1, R2\}), \right. \\
 & \quad \left. (B_2(i) < M_{R2}, \mathbb{O}, (B_1(i) \geq M_{R1}), \overline{\mathbb{G}})\right\}. \tag{119}
 \end{aligned}$$

Let  $\Pr\{B_1(i+1) \leq x\} = G_1^{i+1}(x)$ . With  $i \rightarrow \infty$ , if the energy buffer is in its steady state, it obeys that,  $\Pr\{B_1(i+1) \leq x\} = G_1^{i+1}(x) = G_1^i(x) = G_1(x)$ . In this scenario, Eq. (119) can be written as follows

$$\begin{aligned}
 G_1(x) = & \left[ p_S + p_{SR2} + ((p_1 + p_2 + p_3) * o(1-f))PU2 \right. \\
 & \left. + (p_1 + p_2 + p_3)(1-h) \right] \int_{\mu_1=0}^x F_X(x - \mu_1)g_1(\mu_1) d\mu_1 \\
 & + \left[ p_{SR1} [c * \mathfrak{d}(\Pr\{\gamma_{SR2}(i) \geq \Gamma_{th}\}) \right. \\
 & \quad \left. + \Pr\{\gamma_{SR2}(i) < \Gamma_{th}\} \Pr\{\gamma_{R1R2}(i) < \Gamma_{th}\}) + 1 - c \right] \\
 & + ((p_1 + p_2 + p_3) * \mathfrak{o} * \mathfrak{f} * \mathfrak{g})PU2 \\
 & + ((p_1 + p_2 + p_3) * \mathfrak{o} * \mathfrak{g})(1 - PU2) \\
 & \times \int_{\mu_1=M_{R1}}^x F_X(x - \mu_1)g_1(\mu_1) d\mu_1 \\
 & + \left[ p_{SR1} + PU2((p_1 + p_2 + p_3) * \mathfrak{o} * \mathfrak{f}) \right. \\
 & \quad \left. + (1 - PU2)((p_1 + p_2 + p_3) * \mathfrak{o}) \right] \\
 & \times \int_{\mu_1=0}^{\min(x, M_{R1})} F_X(x - \mu_1)g_1(\mu_1) d\mu_1 \\
 & + \left[ p_{SR1} * c \left( (1 - \mathfrak{d}) + \mathfrak{d} \left( 1 - e^{-W_{SR2}\Gamma_{th}} \right) e^{-W_{R1R2}\Gamma_{th}} \right) \right. \\
 & \quad \left. + PU2((p_1 + p_2 + p_3) * \mathfrak{o} * \mathfrak{f}(1 - \mathfrak{g})) \right. \\
 & \quad \left. + (1 - PU1)((p_1 + p_2 + p_3) * \mathfrak{o}(1 - \mathfrak{g})) \right] \\
 & \times \int_{\mu_1=M_{R1}}^{x+M_{R1}} F_X(x + M_{R1} - \mu_1) d\mu_1, \tag{120}
 \end{aligned}$$

where  $g_1(x)$  is the PDF of  $B_1(i)$ .  $F_X(x) = 1 - e^{-\lambda_1 x}$  is the CDF of  $X$ . By simplifying Eq. (120), we arrive at

$$G_1(x) = \begin{cases} G_{11}(x), & 0 \leq x < M_{R1} \\ G_{12}(x), & x \geq M_{R1} \end{cases} \tag{121}$$

where,

$$G_{11}(x) = \int_{\mu_1=0}^x F_X(x - \mu_1)g_1(\mu_1) d\mu_1 + b_1 \int_{\mu_1=M_{R1}}^{x+M_{R1}} F_X(x + M_{R1} - \mu_1)g_1(\mu_1) d\mu_1, \quad 0 \leq x < M_{R1} \quad (122)$$

$$G_{12}(x) = \int_{\mu_1=0}^{M_{R1}} F_X(x - \mu_1)g_1(\mu_1) d\mu_1 + a_1 \int_{\mu_1=M_{R1}}^x F_X(x - \mu_1)g_1(\mu_1) d\mu_1 + b_1 \int_{\mu_1=M_{R1}}^{x+M_{R1}} F_X(x + M_{R1} - \mu_1)g_1(\mu_1) d\mu_1, \quad x \geq M_{R1} \quad (123)$$

where,

$$a_1 = p_S + p_{SR2} + ((p_1 + p_2 + p_3) * o(1 - f)) * PU2 + (p_1 + p_2 + p_3)(1 - e) + p_{SR1} (c * d(e^{-W_{SR2}\Gamma_{th}} + (1 - e^{-W_{SR2}\Gamma_{th}})(1 - e^{-W_{R1R2}\Gamma_{th}}))) + (1 - c) + ((p_1 + p_2 + p_3) * o * f * g)PU2 + ((p_1 + p_2 + p_3) * o * g)(1 - PU2), \quad (124)$$

$$b_1 = p_{SR1} * c((1 - d) + d(1 - e^{-W_{SR2}\Gamma_{th}}))e^{-W_{R1R2}\Gamma_{th}} + PU2((p_1 + p_2 + p_3) * o * f(1 - g) + (1 - PU2) * ((p_1 + p_2 + p_3) * o(1 - g))). \quad (125)$$

According to Eq. (121), the PDF  $g_1(x)$  may be defined as

$$g_1(x) = \begin{cases} g_{11}(x), & 0 \leq x < M_{R1} \\ g_{12}(x), & x \geq M_{R1}. \end{cases} \quad (126)$$

After substituting Eq. (126) into Eq. (123), the derivatives of Eq. (123) about  $x$  can be obtained

$$g_{12}(x) = \int_{\mu_1=0}^{M_{R1}} f_X(x - \mu_1)g_{11}(\mu_1) d\mu_1 + a_1 \int_{\mu_1=M_{R1}}^x f_X(x - \mu_1)g_{12}(\mu_1) d\mu_1 + b_1 \int_{\mu_1=M_{R1}}^{x+M_{R1}} f_X(x + M_{R1} - \mu_1)g_{12}(\mu_1) d\mu_1, \quad x \geq M_{R1}, \quad (127)$$

Like  $g_{22}(x)$  in Appendix B, let  $g_{12}(x) = k_1e^{Q_1x}$ . Substituting  $g_{12}(x) = k_1e^{Q_1x}$  and  $f_X(x) = \lambda_1e^{-\lambda_1x}$  into Eq. (127), we get

$$k_1e^{Q_1x} = \int_{\mu_1=0}^{M_{R1}} \lambda_1e^{-\lambda_1(x-\mu_1)}g_{11}(\mu_1) d\mu_1 + (1 - b_1) \int_{\mu_1=M_{R1}}^x \lambda_1e^{-\lambda_1(x-\mu_1)}k_1e^{Q_1\mu_1} d\mu_1 + b_1 \times \int_{\mu_1=M_{R1}}^{x+M_{R1}} \lambda_1e^{-\lambda_1(x+M_{R1}-\mu_1)}k_1e^{Q_1\mu_1} d\mu_1, \quad x \geq M_{R1} \quad (128)$$

Simplifying Eq. (128), we have

$$k_1e^{Q_1x} = \lambda_1e^{-\lambda_1x} \int_{\mu_1=0}^{M_{R1}} e^{\lambda_1\mu_1}g_{11}(\mu_1) d\mu_1 - \frac{\lambda_1k_1[b_1 + (1 - b_1)e^{\lambda_1M_{R1}}]}{\lambda_1 + Q_1} e^{(Q_1M_{R1} - \lambda_1x)} + \frac{b_1\lambda_1e^{Q_1M_{R1}} + (1 - b_1)\lambda_1}{\lambda_1 + Q_1} k_1e^{Q_1x}, \quad x \geq M_{R1} \quad (129)$$

In order to ensure  $g_{12}(x) = k_1e^{Q_1x}$ , the coefficients of corresponding terms in Eq. (129) both sides are equal. Thus, we get

$$\begin{cases} \frac{b_1\lambda_1e^{Q_1M_{R1}} + a_1\lambda_1}{\lambda_1 + Q_1} = 1, & (130a) \\ \frac{k_1e^{Q_1M_{R1}}[b_1 + a_1e^{\lambda_1M_{R1}}]}{\lambda_1 + Q_1} = \int_{\mu_1=0}^{M_{R1}} e^{\lambda_1\mu_1}g_{11}(\mu_1) d\mu_1. & (130b) \end{cases}$$

Although, it can be easily found from Eq. (130a) that  $Q_{10} = 0$  is one of the solutions of  $Q_1$  in Eq. (130a),  $Q_{10}$  does not satisfy the condition that  $g_{12}(x)$  is a limiting distribution. And the other solution  $Q_{11}$  of  $Q_1$  in Eq. (130a) can be obtained by simplifying Eq. (130a) as

$$b_1\lambda_1e^{Q_1M_{R1}} = \lambda_1 - a_1\lambda_1 + Q_1 = b_1\lambda_1 + Q_1, \quad (131)$$

With Lambert W function, the solution  $Q_{11}$  can be expressed as follows

$$Q_1 = \frac{-W(-b_1\lambda_1M_{R1}e^{-b_1\lambda_1M_{R1}})}{M_{R1}} - b_1\lambda_1, \quad (132)$$

Due to the property of Lambert W function, when  $b_1\lambda_1M_{R1} \leq 1$ ,  $W(-b_1\lambda_1M_{R1}e^{-b_1\lambda_1M_{R1}}) = -b_1\lambda_1M_{R1}$ , as a result,  $Q_{11} = Q_{10} = 0$ . On the other hand, when  $b_1\lambda_1M_{R1} > 1$ ,  $W(-b_1\lambda_1M_{R1}e^{-b_1\lambda_1M_{R1}}) > -b_1\lambda_1M_{R1}$  so that  $Q_{11} < 0$ , ensuring the limiting distribution of  $g_{12}(x)$ . Thus, for the stationary distribution of  $g_{12}(x)$ , we obtain

$$Q_1 = \frac{-W(-b_1\lambda_1M_{R1}e^{-b_1\lambda_1M_{R1}})}{M_{R1}} - b_1\lambda_1, \quad b_1\lambda_1M_{R1} > 1. \quad (133)$$

Similarly, when  $0 \leq x < M_{R1}$ , substituting Eq. (126) into Eq. (122), the derivatives of Eq. (122) about  $x$  can be obtained

$$g_{11}(x) = b_1 \int_{\mu_1=M_{R1}}^{x+M_{R1}} f_X(x + M_{R1} - \mu_1)g_{12}(\mu_1) d\mu_1 + \int_{\mu_1=0}^x f_X(x - \mu_1)g_{11}(\mu_1) d\mu_1, \quad 0 \leq x < M_{R1} \quad (134)$$

Substituting  $g_{12}(x) = k_1 e^{Q_1 x}$  and  $f_X(x) = \lambda_1 e^{-\lambda_1 x}$  into Eq. (134), we get

$$g_{11}(x) = \lambda_1 \int_{\mu_1=0}^x e^{-\lambda_1(x-\mu_1)} g_{11}(\mu_1) d\mu_1 + \frac{b_1 k_1 \lambda_1 e^{Q_1 M_{R1}}}{\lambda_1 + Q_1} (e^{Q_1 x} - e^{-\lambda_1 x}), 0 \leq x < M_{R1} \quad (135)$$

Similar to  $g_{21}(x)$  in Appendix B, the solution of  $g_{11}(x)$  may be given as follows

$$g_{11}(x) = \frac{b_1 k_1 \lambda_1 e^{Q_1 M_{R1}}}{\lambda_1 + Q_1} (e^{Q_1 x} - e^{-\lambda_1 x}) + \lambda_1 \int_{t=0}^x \frac{b_1 k_1 \lambda_1 e^{Q_1 M_{R1}}}{\lambda_1 + Q_1} (e^{Q_1 t} - e^{-\lambda_1 t}) dt = \frac{b_1 k_1 \lambda_1 e^{Q_1 M_{R1}} (e^{Q_1 x} - 1)}{Q_1}, 0 \leq x < M_{R1} \quad (136)$$

According to the unit area condition on  $g_1(x)$ , we have

$$\int_{x=0}^{\infty} g_1(x) dx = \int_{x=0}^{M_{R1}} g_{11}(x) dx + \int_{x=M_{R1}}^{\infty} g_{12}(x) dx = 1, \quad (137)$$

Substituting  $g_{11}(x) = \frac{b_1 k_1 \lambda_1 e^{Q_1 M_{R1}} (e^{Q_1 x} - 1)}{Q_1}$  and  $g_{12}(x) = k_1 e^{Q_1 x}$  into Eq. (137), we get

$$\frac{b_1 k_1 \lambda_1 e^{Q_1 M_{R1}}}{Q_1} \int_{x=0}^{M_{R1}} (e^{Q_1 x} - 1) dx + k_1 \int_{x=M_{R1}}^{\infty} e^{Q_1 x} dx = 1, \quad (138)$$

Simplifying Eq. (138), we have

$$\frac{b_1 k_1 \lambda_1 e^{Q_1 M_{R1}}}{Q_1} \left[ \frac{e^{Q_1 M_{R1}} - 1}{Q_1} - M_{R1} \right] - \frac{k_1 e^{Q_1 M_{R1}}}{Q_1} = 1, \quad (139)$$

Substituting Eq. (131) into Eq. (139), then simplifying Eq. (139), the value of  $k_1$  can be obtained as follows

$$k_1 = \frac{-Q_1}{M_{R1} (b_1 \lambda_1 + Q_1)}, \quad (140)$$

Substituting Eq. (131) and Eq. (140) into Eq. (136), we arrive at

$$g_{11}(x) = \frac{1 - e^{Q_1 x}}{M_{R1}}. \quad (141)$$

Substituting Eq. (141) into the right side of Eq. (130b), we obtain

$$\int_{\mu_1=0}^{M_{R1}} e^{\lambda_1 \mu_1} g_{11}(\mu_1) d\mu_1 = \int_{\mu_1=0}^{M_{R1}} \frac{(1 - e^{Q_1 x}) e^{\lambda_1 \mu_1}}{M_{R1}} d\mu_1 = \frac{1 - e^{(\lambda_1 + Q_1) M_{R1}}}{(\lambda_1 + Q_1) M_{R1}} - \frac{1 - e^{\lambda_1 M_{R1}}}{\lambda_1 M_{R1}}, \quad (142)$$

The equation in Eq. (131) leads us to conclude  $\lambda_1 M_{R1} = \frac{(\lambda_1 + Q_1) M_{R1}}{b_1 e^{Q_1 M_{R1}} + a_1}$ . Substituting this conclusion in Eq. (142), we have

$$\int_{\mu_1=0}^{M_{R1}} e^{\lambda_1 \mu_1} g_{11}(\mu_1) d\mu_1 = \frac{(1 - e^{Q_1 M_{R1}})(b_1 + a_1 e^{\lambda_1 M_{R1}})}{(\lambda_1 + Q_1) M_{R1}}, \quad (143)$$

Similarly, the conclude  $1 - e^{Q_1 M_{R1}} = \frac{-Q_1}{b_1 \lambda_1}$  may be obtained from Eq. (131). Substituting this conclusion in Eq. (143), we arrive at

$$\int_{\mu_1=0}^{M_{R1}} e^{\lambda_1 \mu_1} g_{11}(\mu_1) d\mu_1 = \frac{-Q_1 (b_1 + a_1 e^{\lambda_1 M_{R1}})}{(\lambda_1 + Q_1) M_{R1} b_1 \lambda_1} = \frac{-Q_1 e^{Q_1 M_{R1}} (b_1 + a_1 e^{\lambda_1 M_{R1}})}{(\lambda_1 + Q_1) M_{R1} b_1 \lambda_1 e^{Q_1 M_{R1}}} = \frac{-Q_1 e^{Q_1 M_{R1}} (b_1 + a_1 e^{\lambda_1 M_{R1}})}{M_{R1} (b_1 \lambda_1 + Q_1) (\lambda_1 + Q_1)} = \frac{k_1 e^{Q_1 M_{R1}} (b_1 + a_1 e^{\lambda_1 M_{R1}})}{\lambda_1 + Q_1}. \quad (144)$$

Now, it can be shown that  $g_{11}(x)$  satisfies the condition in Eq. (130b). Therefore, there is no doubt that the unique solution  $g_{11}(x)$  in Eq. (141) for Eq. (134) and the unique solution  $g_{12}(x) = k_1 e^{Q_1 x}$  for Eq. (127) are obtained.

## REFERENCES

- [1] M.-L. Ku, W. Li, Y. Chen, and K. J. R. Liu, "Advances in energy harvesting communications: Past, present, and future challenges," *IEEE Commun. Surveys Tuts.*, vol. 18, no. 2, pp. 1384–1412, 2nd Quart., 2016.
- [2] J. Ramis-Bibiloni and L. Carrasco-Martorell, "Energy harvesting effect on the sensors battery lifespan of an energy efficient SmartBAN network," in *Proc. Int. Wireless Commun. Mobile Comput. (IWCMC)*, 2021, pp. 1593–1598.
- [3] D. Sui, F. Hu, W. Zhou, M. Shao, and M. Chen, "Relay selection for radio frequency energy-harvesting wireless body area network with buffer," *IEEE Internet Things J.*, vol. 5, no. 2, pp. 1100–1107, Apr. 2018.
- [4] A. Alsharoa, H. Ghazzai, A. E. Kamal, and A. Kadri, "Optimization of a power splitting protocol for two-way multiple energy harvesting relay system," *IEEE Trans. Green Commun. Netw.*, vol. 1, no. 4, pp. 444–457, Dec. 2017.
- [5] Y. Zou, J. Zhu, and X. Jiang, "Joint power splitting and relay selection in energy-harvesting communications for IoT networks," *IEEE Internet Things J.*, vol. 7, no. 1, pp. 584–597, Jan. 2020.
- [6] R. Morsi, D. S. Michalopoulos, and R. Schober, "ON-OFF transmission policy for wireless powered communication with energy storage," in *Proc. 48th Asilomar Conf. Signals Syst. Comput.*, 2014, pp. 1676–1682.
- [7] R. Morsi, D. S. Michalopoulos, and R. Schober, "Performance analysis of near-optimal energy buffer aided wireless powered communication," *IEEE Trans. Wireless Commun.*, vol. 17, no. 2, pp. 863–881, Feb. 2018.
- [8] Y. Wu, L. P. Qian, L. Huang, and X. Shen, "Optimal relay selection and power control for energy-harvesting wireless relay networks," *IEEE Trans. Green Commun. Netw.*, vol. 2, no. 2, pp. 471–481, Jun. 2018.
- [9] X. Lan, Q. Chen, L. Cai, and L. Fan, "Buffer-aided adaptive wireless powered communication network with finite energy storage and data buffer," *IEEE Trans. Wireless Commun.*, vol. 18, no. 12, pp. 5764–5779, Dec. 2019, doi: [10.1109/TWC.2019.2938958](https://doi.org/10.1109/TWC.2019.2938958).
- [10] D. Bapatla and S. Prakriya, "Performance of energy-buffer aided incremental relaying in cooperative networks," *IEEE Trans. Wireless Commun.*, vol. 18, no. 7, pp. 3583–3598, Jul. 2019.

[11] D. Bapatla and S. Prakriya, "Performance of a cooperative communication network with green self-sustaining nodes," *IEEE Trans. Green Commun. Netw.*, vol. 5, no. 1, pp. 426–441, Mar. 2021.

[12] D. Bapatla and S. Prakriya, "Performance of networks with an energy buffer-aided source and a data buffer-aided relay," in *Proc. IEEE 31st Annu. Int. Symp. Pers. Indoor Mobile Radio Commun.*, London, U.K., 2020, pp. 1–5.

[13] V. P. Tuan, S. Q. Nguyen, and H. Y. Kong, "Performance analysis of energy-harvesting relay selection systems with multiple antennas in presence of transmit hardware impairments," in *Proc. Int. Conf. Adv. Technol. Commun. (ATC)*, 2016, pp. 126–130.

[14] B. S. Awoyemi, A. S. Alfa, and B. T. Maharaj, "Network restoration in wireless sensor networks for next-generation applications," *IEEE Sensors J.*, vol. 19, no. 18, pp. 8352–8363, Sep. 2019.

[15] W. Lu et al., "OFDM based bidirectional multi-relay SWIPT strategy for 6G IoT networks," *China Commun.*, vol. 17, no. 12, pp. 80–91, Dec. 2020.

[16] N. Chakchouk, "A survey on opportunistic routing in wireless communication networks," *IEEE Commun. Surveys Tuts.*, vol. 17, no. 4, pp. 2214–2241, 4th Quart., 2015.

[17] J. Zuo, C. Dong, S. X. Ng, L. Yang, and L. Hanzo, "Cross-layer aided energy-efficient routing design for ad hoc networks," *IEEE Commun. Surveys Tuts.*, vol. 17, no. 3, pp. 1214–1238, 3rd Quart., 2015.

[18] J. Zuo, C. Dong, H. V. Nguyen, S. X. Ng, L. Yang, and L. Hanzo, "Cross-layer aided energy-efficient opportunistic routing in ad hoc networks," *IEEE Trans. Commun.*, vol. 62, no. 2, pp. 522–535, Feb. 2014.

[19] W. An, C. Dong, X. Xu, C. Xu, S. Han, and L. Teng, "Opportunistic routing-aided cooperative communication network with energy harvesting," *IEEE Internet Things J.*, vol. 10, no. 8, pp. 6928–6945, Apr. 2023.

[20] Z. Chen, J. Yuan, and B. Vucetic, "Analysis of transmit antenna selection/maximal-ratio combining in Rayleigh fading channels," *IEEE Trans. Veh. Technol.*, vol. 54, no. 4, pp. 1312–1321, Jul. 2005.

[21] S. Luo, R. Zhang, and T. J. Lim, "Optimal save-then-transmit protocol for energy harvesting wireless transmitters," *IEEE Trans. Wireless Commun.*, vol. 12, no. 3, pp. 1196–1207, Mar. 2013.

[22] B. Zhang, C. Dong, M. El-Hajjar, and L. Hanzo, "Outage analysis and optimization in single- and multiuser wireless energy harvesting networks," *IEEE Trans. Veh. Technol.*, vol. 65, no. 3, pp. 1464–1476, Mar. 2016.

[23] A. Polyanin and A. Manzhirov, *Handbook of Integral Equations: Second Edition* (Handbooks of Mathematical Equations). London, U.K.: Taylor & Francis, 2008.

[24] R. Loynes, "The stability of a queue with non-independent inter-arrival and service times," *Math. Proc. Cambridge Philos. Soc.*, vol. 58, no. 3, pp. 497–520, Jul. 1962.

[25] D. Bapatla and S. Prakriya, "Performance of two-hop links with an energy buffer-aided IoT source and a data buffer-aided relay," *IEEE Internet Things J.*, vol. 8, no. 6, pp. 5045–5061, Mar. 2021.



**LEI TENG** is currently pursuing the bachelor's degree in information and communication engineering from the Beijing University of Posts and Telecommunications, Beijing, China.

His research interests include cooperative communications, energy harvesting, and opportunistic routing.



**WANNIAN AN** received the M.Sc. degree in information and communication engineering from Shenzhen University, Shenzhen, China, in 2021. He is currently pursuing the Ph.D. degree in information and communication engineering with the Beijing University of Posts and Telecommunications, Beijing, China.

His research interests include cooperative communications, energy harvesting, opportunistic routing, and semantic communication.



**CHEN DONG** received the B.S. degree in electronic information sciences and technology from the University of Science and Technology of China, Hefei, China, in 2004, the M.Eng. degree in pattern recognition and automatic equipment from the University of Chinese Academy of Sciences, Beijing, China, in 2007, and the Ph.D. degree from the University of Southampton, U.K., in 2014.

He was a Postdoctoral Research Fellow with the University of Southampton. He used to work with Huawei Device Company Ltd., China. Since 2020, he has been working with the Beijing University of Posts and Telecommunications. His research interests include applied math, relay system, channel modeling, and cross-layer optimization. He was a recipient of the Best Paper Award at the IEEE VTC 2014.



**XIAODONG XU** (Senior Member, IEEE) received the B.S. degree in information and communication engineering and the master's degree in communication and information system from Shandong University in 2001 and 2004, respectively, and the Ph.D. degree in circuit and system from the Beijing University of Posts and Telecommunications (BUPT) in 2007.

He is currently a Professor with BUPT and a Research Fellow with Peng Cheng Laboratory. He has coauthored nine books and more than 120 journal and conference papers. He is also the inventor or co-inventor of 51 granted patents. His research interests cover semantic communications, moving networks, mobile edge computing, and caching.



**BOXIAO HAN** received the M.A.Sc. degree in electrical and computer engineering from McMaster University, Canada. Since 2018, he has been working as a Researcher with China Mobile Research Institute. His expertise lies in digital signal processing, heterogeneous computing, and cloud computing. His current research interests include 6G prototype design and cloud-based RAN platform. He has also been a representative for 3GPP RAN4 and O-RAN.